STEM CELLS®
TISSUE-SPECIFIC STEM CELLS

Oxygen Levels Epigenetically Regulate Fate Switching of Neural Precursor Cells via Hypoxia-Inducible Factor 1α-Notch Signal Interaction in the Developing Brain

TETSUJI MUTOH, TSUKASA SANOSAKA, KEI ITO, KINICHI NAKASHIMA

Laboratory of Molecular Neuroscience, Graduate School of Biological Sciences, Nara Institute of Science and Technology, Ikoma, Nara, Japan

Key Words. Neural precursor cell • Astrocyte differentiation • DNA methylation • Epigenetic gene regulation • Notch signaling • Oxygen concentration

ABSTRACT

Oxygen levels in tissues including the embryonic brain are lower than those in the atmosphere. We reported previously that Notch signal activation induces demethylation of astrocytic genes, conferring astrocyte differentiation ability on midgestational neural precursor cells (mgNPCs). Here, we show that the oxygen sensor hypoxia-inducible factor 1α (HIF1α) plays a critical role in astrocytic gene demethylation in mgNPCs by cooperating with the Notch signaling pathway. Expression of constitutively active HIF1α and a hyperoxic environment, respectively, promoted and impeded astrocyte differentiation in the developing brain. Our findings suggest that hypoxia contributes to the appropriate scheduling of mgNPC fate determination. STEM CELLS *2012;30:561–569*

Disclosure of potential conflicts of interest is found at the end of this article.

INTRODUCTION

The mammalian embryonic brain contains multipotent neural precursor cells (NPCs) that can self-renew and give rise to all three major cell types in the nervous system, that is, neurons, astrocytes, and oligodendrocytes. NPC fate determination is regulated by the collaboration between cell-external cues, from molecules such as cytokines and growth factors, and cell-internal epigenetic programs [1].

We and others have shown that members of the interleukin-6 (IL-6) family of cytokines, including leukemia inhibitory factor (LIF), efficiently induce astrocyte differentiation of late-gestational (lg) NPCs by activating the janus kinase (JAK)-signal transducer and activator of transcription (STAT) signaling pathway [2, 3]. In contrast to lgNPCs, midgestational (mg) NPCs differentiate only into neurons because the promoters of astrocytic genes, such as that encoding the typical astrocytic marker glial fibrillary acidic protein (GFAP), are hypermethylated at this stage [4, 5]. These findings indicate that DNA methylation is a critical determinant for the acquisition of astrocyte differentiation ability by NPCs [6]. Notch receptors and their ligands, molecules best known for influencing cell fate decisions through direct cell-cell contact, participate in a wide variety of biological processes, including fate determination of NPCs. As gestation proceeds, mgNPCs generate committed neuronal precursors (or young neurons) expressing Notch ligands, and these cells activate Notch signaling in neighboring NPCs. Notch signal activation induces the demethylation of astrocytic gene promoters in NPCs, which explains, at least in part, how the neuronal-to-glial cell fate switch occurs in NPCs during brain development [1, 6, 7].

Oxygen is essential for cell survival as the final electron acceptor in the electron transport chain of aerobic respiration. Sensing and controlling oxygen localization are of extreme importance because normal metabolic processes generate radical intermediates. When oxygen levels exceed the capacity of endogenous antioxidant systems, radicals including reactive oxygen species attack cellular components such as nucleic acids, the sulfhydryl groups of proteins, or the unsaturated fatty acid moieties of phospholipids [8].

Hypoxia-inducible factors (HIFs) are known to play critical roles as molecular sensors of oxygen tension. HIF1α activity in cells is controlled by oxygen levels in multiple ways, such as transcriptional regulation and hydroxylation-dependent binding by Von Hippel-Lindau tumor suppressor protein followed by proteasomal degradation [9–11]. A HIF1 complex composed of HIF1α and HIF1β (also known as ARNT) binds to the hypoxia response element and activates the transcription of target genes such as *inhibitor of differentiation 2* [12], *insulin-like growth factor binding protein, p21, phosphoglycerate kinase 1*, and *vascular endothelial growth factor* [13].

Author contribution: T.M.: conception and design, financial support, administrative support, provision of study material or patients, collection and/or assembly of data, data analysis and interpretation, and manuscript writing; T.S.: administrative support, collection and/or assembly of data, and data analysis and interpretation; K.I.: provision of study material or patients; and K.N.: conception and design, financial support, administrative support, data analysis and interpretation, and final approval of manuscript. T.M. and T.S. contributed equally to this study.

Correspondence: Kinichi Nakashima, Ph.D., Laboratory of Molecular Neuroscience, Graduate School of Biological Sciences, Nara Institute of Science and Technology, Ikoma, Nara 630-0192, Japan. Telephone: 81-743-72-5471; Fax: 81-743-72-5479; e-mail: kin@bs.naist.jp Received July 19, 2011; accepted for publication December 2, 2011; first published online in STEM CELLS *EXPRESS* December 29, 2011. 1066-5099/2011/$30.00/0 doi: 10.1002/stem.1019

HIF1α has also been reported to be crucial for normal brain development [14]. Moreover, HIFs may act cooperatively with other signaling molecules, such as Notch [15] and mammalian target of rapamycin [16, 17], thereby influencing a wide range of processes including tumor malignancy and NPC growth, maintenance and differentiation [11, 18-20].

In this study, we focused on how oxygen tension affects the DNA methylation status of astrocytic genes in mgNPCs. Oxygen levels in the microenvironment around NPCs in the embryonic brain at midgestation were comparable to those seen under hypoxic culture conditions (2-5% O_2). Bisulfite sequencing revealed that these conditions promoted demethylation of the *gfap* promoter. This hypoxia-induced demethylation was mediated by cooperation between HIF1α and the Notch signaling pathway. Furthermore, ectopic expression of a constitutively active form of HIF1α in the embryonic brain induced precocious astrocyte differentiation of NPCs. By contrast, when embryos developed in hyperoxic conditions, astrocyte differentiation of NPCs was suppressed. These findings suggest that oxygen levels in the embryonic brain play a critical role in fine-tuning the timing of NPC fate switching during development.

Materials and Methods

Cell Culture

mgNPCs were prepared from telencephalons of E11.5 embryos and cultured as described previously [5]. E15.5 ventricular zone (VZ) containing NPCs was manually separated from other parts of the brain using a hand-made microknife (Supporting Information Fig. S1). As described previously [5], NPCs were cultured with basic fibroblast growth factor (bFGF; 1×10^6 cells per dish) in poly-L-ornithine/fibronectin-coated 6-cm culture dishes. Hand-made chambers were used to obtain atmospheres of different oxygen levels [21]. Notch signal activation was inhibited with the γ-secretase inhibitor *N*-[*N*-(3,5-difluorophenacetyl-L-alanyl)]-*S*-phenylglycine *t*-butyl ester (DAPT; Calbiochem-MERCK, Darmstadt, Germany, www.merckgroup.com, 10 μM).

Bisulfite Sequencing

Genomic DNA was extracted from NPCs and subjected to bisulfite sequencing as previously described [5]. Specific DNA fragments were amplified by polymerase chain reaction (PCR) using primers described previously [5, 7]. The PCR products were cloned into pT7Blue vector (Novagen, Darmstadt, Germany, www.merckgroup.com/en/index.html), and 10-20 randomly picked clones were sequenced. Each experiment was performed at least tree times.

Lentivirus Production

A mouse *HIF1α*-targeting short hairpin RNA (shRNA) sequence [22] was cloned into pLLX vector [23]. Lentiviruses were pseudotyped with the vesicular somatitis virus–G envelope and concentrated by centrifugation as previously described [24]. *HIF1α* mRNA degradation was confirmed by quantitative PCR (qPCR). All the recombinant DNA experiments in this manuscript followed the guidelines by Ministry of Education, Culture, Sports, Science and Technology of Japan, which conform to the National Institutes of Health Guidelines.

Immunostaining

Cells were fixed with 4% paraformaldehyde and processed for immunostaining as described [5]. The following primary antibodies were used: chick anti-green fluorescent protein (anti-GFP; 1:500, Aves Labs, Tigard, OR, www.aveslab.com), rat anti-hemagglutinating (anti-HA) (1:500, Roche Applied Science, Indianapolis, IN, www.roche-applied-science.com), rat anti-bromodeoxyuridine (1:250, AbD Serotec, Raleigh, NC, www.abdserotec.com) chicken anti-Nestin (1:1000, Aves Labs), mouse anti-Map2ab (1:500, Sigma, St. Louis, MO, www.sigmaaldrich.com), and mouse anti-GFAP (1:500, Sigma). Secondary antibodies were Alexa488-conjugated goat anti-rat IgG (1:500), Alexa488-conjugated goat anti-chick IgY (1:500), Alexa555-conjugated goat anti-rabbit IgG (1:500), Alexa555-conjugated goat anti-rat IgG (1:500), Alexa555-conjugated goat anti-mouse IgG (1:500), or Alexa647-conjugated goat anti-mouse IgG (1:500, Invitrogen, Carlsbad, CA, www.invitrogen.com). Nuclei were stained using bisbenzimide H33258 fluorochrome trihydrochloride (Hoechst; Nacalai Tesque, Kyoto, Japan, www.nacalai.co.jp). All experiments were independently replicated at least three times. A Hypoxyprobe-1 Plus kit (Hypoxyprobe-Millipore, Billerica, MA, www.millipore.com) was used, following the manufacturer's protocol, to determine the hypoxicity of cultured cells and the developing brain. After culturing NPCs for 4 days in 2%, 5%, or 21% O_2, pimonidazole-HCl was added to the culture medium for 1.5 hours and the cells were then fixed. For brain sections, pimonidazole-HCl was injected intraperitoneally into pregnant mice (E15.5). Embryos were fixed 2 hours later with 4% paraformaldehyde and the brains were cryosectioned at 20-μm intervals. Pimonidazole adducts were detected with a fluorescein isothiocyanate–conjugated specific antibody supplied with the kit (1:500). Stained sections were visualized with a confocal microscope (Fluoview FV10i, Olympus, Tokyo, Japan, www.olympus.co.jp) or a fluorescence microscope (Zeiss Axiovert 200M, Zeiss, Jena, Germany, www.zeiss.com).

Animal Procedures and Electroporation

All aspects of animal care and treatment were conducted according to the guidelines of the Experimental Animal Care Committee of Nara Institute of Science and Technology. The surgical procedures performed on pregnant ICR mice and embryo manipulations in utero were conducted as previously described [25]. E11.5 pregnant mice were deeply anesthetized by intraperitoneal injection with sodium pentobarbitone (50 μg/g b.wt.). HA–constitutively active HIF1α (HA-caHIF1α) cDNA was cloned into the EcoRI site of pCAGGS vector. After the uterus was exposed, approximately 1-2 μl of plasmid solution (1 μg/μl in phosphate-buffered saline) was injected into the lateral ventricle of the telencephalon with a glass micropipette. The embryos were held with the tips of a tweezers-type electrode with a diameter of 5 mm (CUY650-P3; Tokiwa Science, Fukuoka, Japan), and five electronic pulses (27V, 50 ms, at intervals of 950 ms) were given to each embryo with an electroporator (CUY21SC; Tokiwa Science). The embryos were reinserted into the abdominal cavity and the abdominal wall was closed with surgical sutures.

Exposure to High-Oxygen Atmosphere and Tissue Oxygen Measurement

The animal cage was placed in a hyperoxic oxygen chamber (Terucom, Kanagawa, Japan, www.terucom.co.jp). Oxygen tension was measured using a portable oxygen meter (Terucom) in the same chamber. E11.5 pregnant mice were exposed to 60% O_2 for 2 days, and the oxygen tension was then raised to 80% (the upper nonlethal concentration limit) and maintained at that level until fixation at E17.5.

Local tissue oxygen tension corresponding to each atmospheric oxygen level was measured with an OxyLab pO_2 monitor (Oxford Optronix, Oxford, UK, www.oxford-optronix.com) [26] (Supporting Information Fig. S4Q). The probe was

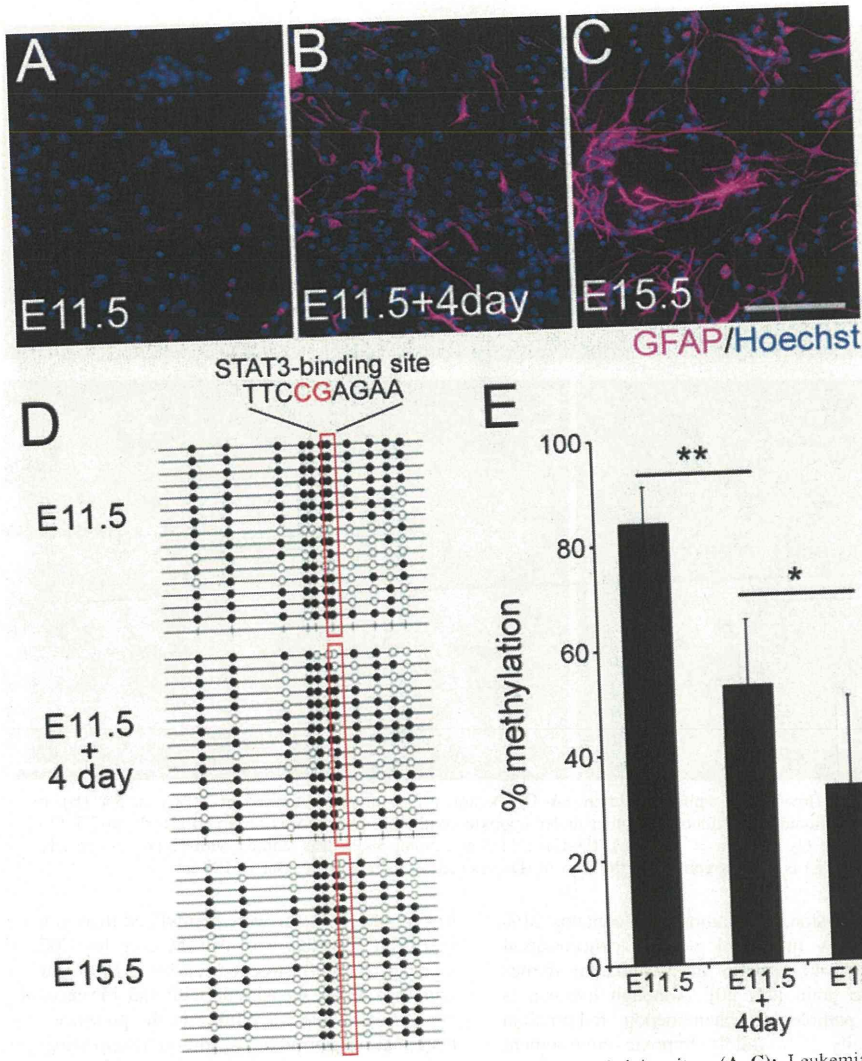

Figure 1. Astrocyte differentiation of midgestational neural precursor cells is retarded in vitro. **(A–C):** Leukemia inhibitory factor (LIF)-induced GFAP-positive astrocyte differentiation in E11.5 (A), in vitro 4-day-cultured E11.5 (B) and E15.5 (C) NPCs. After a 4-day culture in the presence of LIF, the cells were stained with anti-GFAP antibody (magenta) and with Hoechst to identify nuclei (blue). Scale bar = 100 μm. **(D, E):** Genomic DNA was extracted from the cells, and the methylation status of the *gfap* promoter around the STAT3-binding site was examined by bisulfite sequencing. Closed and open circles indicate methylated and unmethylated CpG sites, respectively (D). E11.5 and E15.5 indicate the results obtained for freshly prepared neural precursor cells (NPCs) from E11.5 cortex and E15.5 VZ. The STAT3-binding site is marked by red rectangles. Methylation at the STAT3-binding site in the *gfap* promoter is higher in 4-day in vitro-cultured E11.5 NPCs than in freshly prepared E15.5 NPCs (E). Data are shown as means ± SD ($n = 3$). Statistical significance was evaluated by the Student's t test. *, $p < .05$; **, $p < .01$. Abbreviations: GFAP, glial fibrillary acidic protein; STAT3, signal transducer and activator of transcription.

guided to the E15.5 brain using a 20-gauge needle with a plastic canula (Terumo, Tokyo, Japan, www.terumo.co.jp).

Results

It is well known that lgNPCs but not mgNPCs differentiate into astrocytes in response to stimulation with IL-6 family cytokines [2-5, 7]. When we cultured lgNPCs prepared from the VZ of mouse telencephalon at E15.5 (Supporting Information Fig. S1), we observed their LIF-induced astrocyte differentiation, as judged by the expression of the astrocytic marker GFAP (Fig. 1C, 26.8 ± 6.5%). By contrast, hardly any LIF-treated E11.5 mgNPCs differentiated into astrocytes (Fig. 1A). Interestingly, E11.5 mgNPCs cultured in vitro for 4 days (nominally corresponding to E15.5) did undergo astrocyte differentiation (Fig. 1B, 12.2 ± 1.9%), albeit to a lesser extent than E15.5 lgNPCs.

Since an inverse correlation exists between the potential of NPCs to express *gfap* and the methylation status of the *gfap* promoter, which includes a STAT3-binding site [5, 27], we examined whether the in vitro culture conditions of mgNPCs delayed the demethylation of the promoter compared to its demethylation in vivo. Bisulfite sequencing for the *gfap* promoter of E11.5, E11.5 + 4-day culture in vitro, and E15.5 NPCs revealed that this was indeed the case (Fig. 1D, 1E). These data indicate that the in vitro culture conditions retard the demethylation of the astrocytic gene promoter in NPCs.

In terms of the physical conditions surrounding cells, one of the biggest differences between in vitro and in vivo

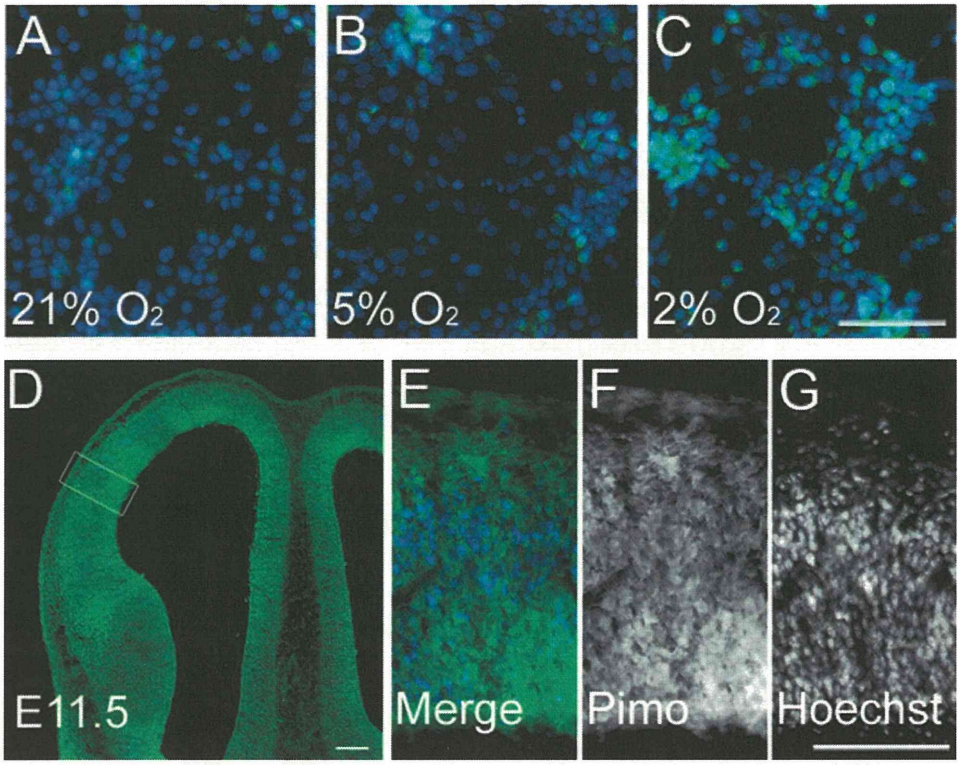

Figure 2. Oxygen levels are low in the embryonic brain. **(A–C):** Neural precursor cells cultured in 21% (A), 5% (B), or 2% O_2 (C) were stained with Hypoxyprobe. Pimonidazole adduct formation under hypoxic conditions (green) was observed clearly in 2% O_2 (C), less markedly in 5% O_2 (B), but not in 21% O_2 (A) (bar = 100 μm). **(D–G):** E11.5 embryonic brain was stained with Hypoxyprobe. Hypoxyprobe (green); Hoechst (blue). The image in (E) is an enlargement of the area in (D) marked by the rectangle. Bar = 100 μm.

environments is oxygen tension. The atmosphere contains 21% O_2 (160 mmHg), whereas interstitial oxygen concentration ranges from 1 to 5% (7-40 mmHg) in mammalian tissues including the embryonic brain [11, 20]. Although hypoxia is generally considered a pathological phenomenon, mammalian embryos develop naturally in a mildly hypoxic environment [28]. To determine the tissue oxygen tension in the embryonic brain, where NPCs reside, we used the chemical reagent pimonidazole. Pimonidazole is reductively activated in hypoxic cells and forms stable adducts with sulfhydryl groups in amino acids, at around or below 10 mmHg, which can be detected with specific antibodies [29, 30]. Pimonidazole adducts were weakly but clearly detected in NPCs cultured in 2% and 5% O_2 conditions, respectively, but not in NPCs cultured in 21% O_2 (Fig. 2A–2C). Pimonidazole adducts were also abundant in midgestational embryonic brain, indicating that oxygen levels there are low, particularly in the NPC-containing VZ (Fig. 2D–2G).

From the above findings, we hypothesized that culturing mgNPCs at a low oxygen level might accelerate their differentiation into astrocytes. To test this idea, mgNPCs were cultured in 2% or 21% O_2 atmospheres for 4 days in the presence of bFGF, and subsequently stimulated with LIF for an additional 4 days. As shown in Figure 3A–3C, a higher proportion of mgNPCs cultured in the presence of LIF under 2% O_2 than under 21% O_2 became GFAP-positive astrocytes. Reflecting the promotion of astrocyte differentiation, NPC (Nestin) and neuron (Map2ab) marker-positive cell numbers were lower under 2% O_2 than under 21% O_2 (Supporting Information Fig. S2A). The proliferation of cells in our normoxic and hypoxic culture was similar as judged by BrdU staining (Supporting Information Fig. S2B). Furthermore, in the 2% O_2 condition, significantly fewer CpG sites in the *gfap* promoter were methylated than in the 21% O_2 condition (Fig. 3D); this was also the case for CpG sites in the promoter of another astrocytic marker, *S100β* (Supporting Information Fig. S3A). Consistent with the lower methylation, *S100β* expression in hypoxic culture in the presence of LIF was higher than that in normoxic condition (Supporting Information Fig. S3B). These results suggest that low oxygen levels facilitate the DNA demethylation of astrocytic genes in mgNPCs.

We have shown previously that Notch signal activation induces the demethylation of astrocytic genes in mgNPCs [7]. Intriguingly, *hairy and enhancer of split 1* (*Hes1*) and *Hes5*, two known targets of Notch signaling, were markedly upregulated in the 2% O_2 culture condition (Fig. 4A), indicating that Notch signaling is more active at lower O_2 levels. Therefore, we examined whether low oxygen levels enhance the astrocyte differentiation of mgNPCs via Notch signal activation. An inhibitor of Notch signal activation, DAPT, was added to the culture medium during the first 4-day expansion phase of mgNPCs with bFGF in the hypoxic condition. The expression of *Hes1* and *Hes5* was dramatically reduced, confirming that hypoxia-induced elevation of Notch signaling was inhibited by DAPT (Supporting Information Fig. S3C). Furthermore, as shown in Figure 4B and 4C, the astrogenic potential of NPCs was almost completely suppressed by DAPT, and the enhanced demethylation of the *gfap* and *S100β* promoters observed in the hypoxic condition was no longer seen after DAPT treatment (Fig. 4D and Supporting Information Fig. S3D).

Activation of the Notch signaling pathway in mgNPCs induces expression of the transcription factor nuclear factor IA (NFIA), which leads to demethylation of astrocyte-specific genes including *gfap* [7]: NFIA binds to astrocytic gene

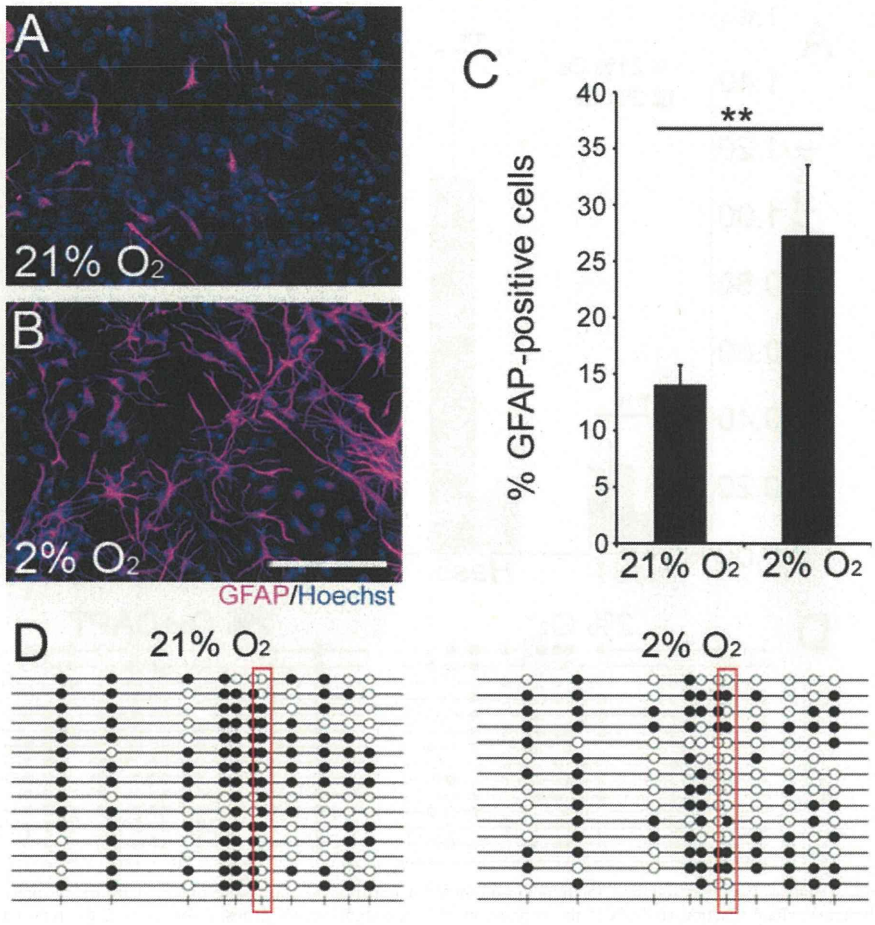

Figure 3. Culturing under 2% O_2 accelerates leukemia inhibitory factor (LIF)-induced astrocyte differentiation of neural precursor cells (NPCs). **(A–C):** E11.5 NPCs were cultured for 4 days under 2% O_2 (A) or 21% O_2 (B), followed by a 4-day LIF stimulation to induce astrocyte differentiation. GFAP (magenta), Hoechst (blue); bar = 100 μm. Proportions of GFAP-positive cells in the total cell populations were quantified (C). Data are shown as means ± SD ($n = 3$). Statistical significance was evaluated by the Student's t test. **, $p < .01$. **(D):** CpG methylation at the signal transducer and activator of transcription 3 (STAT3)-binding site in the *gfap* promoter is lower under 2% O_2 than under 21% O_2 after a 4-day culture of E11.5 NPCs. The STAT3-binding site is indicated by red rectangles. Abbreviation: GFAP, glial fibrillary acidic protein.

promoters and induces dissociation of DNA methyltransferase 1 (DNMT1) from the promoters, resulting in their demethylation. Therefore, we examined the expression of *Nfia* and found that it increased dramatically under the hypoxic condition (Supporting Information Fig. S4A). Moreover, we did not observe astrocyte differentiation of NFIA-deficient NPCs even when cultured with LIF under the hypoxic condition (Supporting Information Fig. S4B). Taken together, these findings suggest that activation of the Notch-NFIA cascade is the mechanism whereby hypoxia induces demethylation of the *gfap* promoter.

HIF1s have been shown to play important roles in cellular adaptation to hypoxia [11, 13, 31]. *HIF1α* and *HIF1β* are expressed in the developing mouse brain [32], and HIF1α protein accumulates to a higher level in hypoxic than in normoxic conditions as a result of increased transcription and protein stabilization [33–35]. Consistent with those observations, we found that both *HIF1α* transcript and nuclear HIF1α protein levels in E11.5 mgNPCs were upregulated under the 2% O_2 culture condition (Supporting Information Fig. S5A, S5B). Expression of the HIF1α target gene *Id1* was also upregulated (Supporting Information Fig. S5C), as was observed in neuroblastoma cells [12].

To determine whether HIF1α contributes to the hypoxia-promoted astrogenic potential of mgNPCs, we suppressed *HIF1α* mRNA using a specific shRNA. mgNPCs were prepared from E11.5 telencephalon and were infected the following day with lentiviruses expressing *HIF1α*-shRNA, cultured under 2% O_2 for 3 days, and then stimulated with LIF for a further 4 days. The level of *HIF1α* mRNA was reduced greatly in cells infected with *HIF1α* shRNA-expressing viruses (Supporting Information Fig. S6A). Moreover, *HIF1α* shRNA expression markedly diminished both the astrogenic potential of mgNPCs and the degree of demethylation in the *gfap* promoter (Fig. 5A–5G, and Supporting Information Fig. S6B).

caHIF1α is a hydroxylation-resistant, constitutively active mutant form of HIF1α in which two amino acids (prolines 402 and 564) are substituted with alanines [36]. One-day in vitro-cultured E11.5 mgNPCs were infected with lentiviruses expressing HA-tagged caHIF1α (HA-caHIF1α) and cultured for a further day, and then subjected to LIF stimulation for 3 days under the normoxic condition. HA-caHIF1α protein was clearly detected in the nucleus (Fig. 5M). In contrast to control virus-infected mgNPCs (Fig. 5H–5K), cells transduced to express HA-caHIF1α became GFAP-positive astrocytes in response to LIF stimulation, even under the 21% O_2 condition

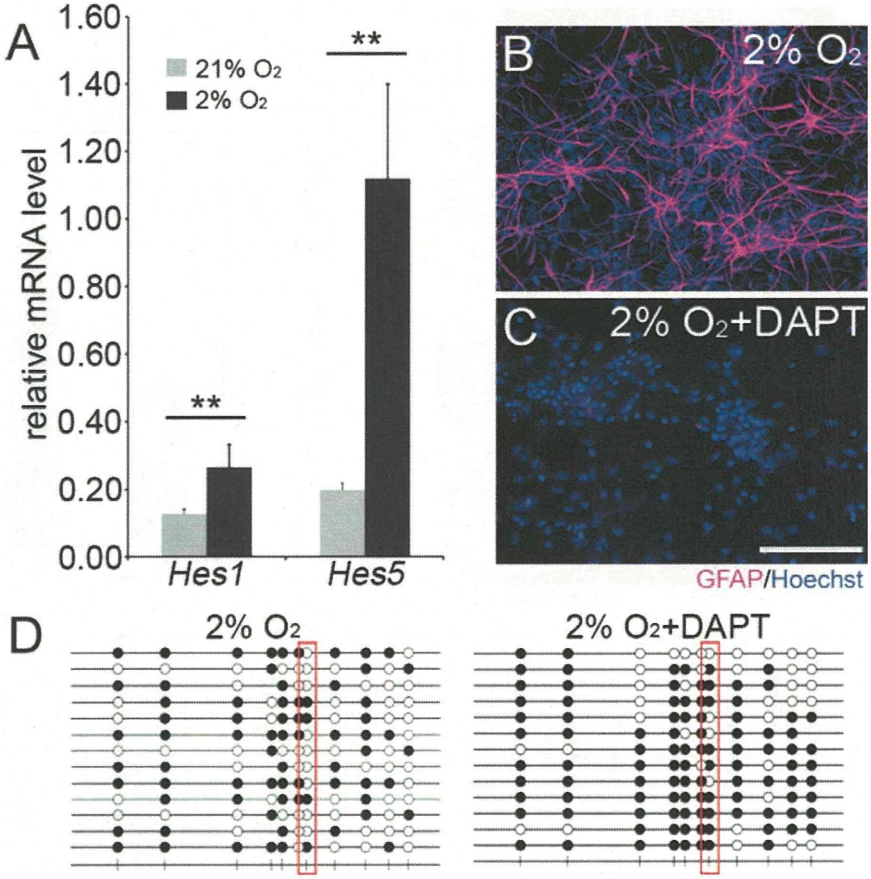

Figure 4. Notch signal activation is required for hypoxia-promoted acquisition of astrogenic potential by neural precursor cells (NPCs). **(A):** Quantitative polymerase chain reaction analysis of the expression of Notch signal target genes. Expression of the representative Notch signal targets *Hes1* and *Hes5* was upregulated in midgestational neural precursor cells cultured for 4 days under 2% O_2. Statistical significance was evaluated by the Student's *t* test. **, $p < .01$. **(B, C):** Hypoxia-induced astrogenic potential of NPCs was blocked by Notch signal inhibition. E11.5 NPCs were cultured for 4 days in the 2% O_2 condition with or without DAPT (10 μM), followed by a 4-day leukemia inhibitory factor stimulation. Bar = 100 μm. **(D):** The methylation status of the *gfap* promoter in E11.5 NPCs cultured with or without DAPT (10 μM) in the 2% O_2 condition was examined by bisulfite sequencing. The signal transducer and activator of transcription 3-binding site is indicated by red rectangles. Abbreviations: DAPT, *N*-[*N*-(3,5-difluorophenacetyl-L-alanyl)]-*S*-phenylglycine *t*-butyl ester); GFAP, glial fibrillary acidic protein.

(Fig. 5L–5O). HA-caHIF1α expression also augmented Notch signal activation in these cells (Fig. 5P). Furthermore, HA-caHIF1α-induced astrocyte differentiation and Notch signal activation were both abolished by DAPT treatment (Fig. 5P and Supporting Information Fig. S6C–S6J). Consistent with the results of these in vitro experiments, ectopic expression of HA-caHIF1α in E11.5 brains led to precocious GFAP expression in NPCs (Supporting Information Fig. S6K–S6P). These experiments suggest that HIF1α promotes the astrogenic potential of mgNPCs by enhancing Notch signal activation, probably because hypoxia-stabilized HIF1α can form a complex with the Notch intracellular domain (NICD) to effectively induce the expression of Notch-target genes [15].

Given that the 21% O_2 condition delayed the acquisition of astrocyte differentiation ability by NPCs in vitro, we next asked whether a hyperoxic environment has a similar effect on NPCs in vivo. To address this, pregnant mice were housed in a normoxic or hyperoxic chamber for 6 days (E11.5 to E17.5). To confirm that the embryonic brain was indeed under hyperoxia, we measured the local brain oxygen tension at E15.5 using an oxygen electrode. When the pregnant mice were in the normoxic (21% O_2) and hyperoxic (80% O_2) conditions, the oxygen tensions were 5.24 and 112.9 mmHg, respectively (Supporting Information Fig. S6Q), indicating that local brain oxygen tension was increased as a result of the atmospheric oxygen levels surrounding the pregnant mother mouse. After 6 days of hyperoxic housing, embryonic brains were then subjected to immunostaining and Western blotting. Interestingly, as shown in Figure 5Q–5S, exposure to high oxygen markedly decreased GFAP expression in the brains of embryos of mice housed in the hyperoxic condition.

These results suggest that a hypoxic environment is important for the proper timing of astrocyte differentiation during embryonic development.

Discussion

HIF1α is known to be an important factor in the response of various types of cells to hypoxic stress such as ischemia [11, 13] and to play a critical role in normal brain development [14]. In the present study, we have shown that astrocytic genes are progressively demethylated in the mildly hypoxic environment of the developing brain (Figs. 1–3). We further

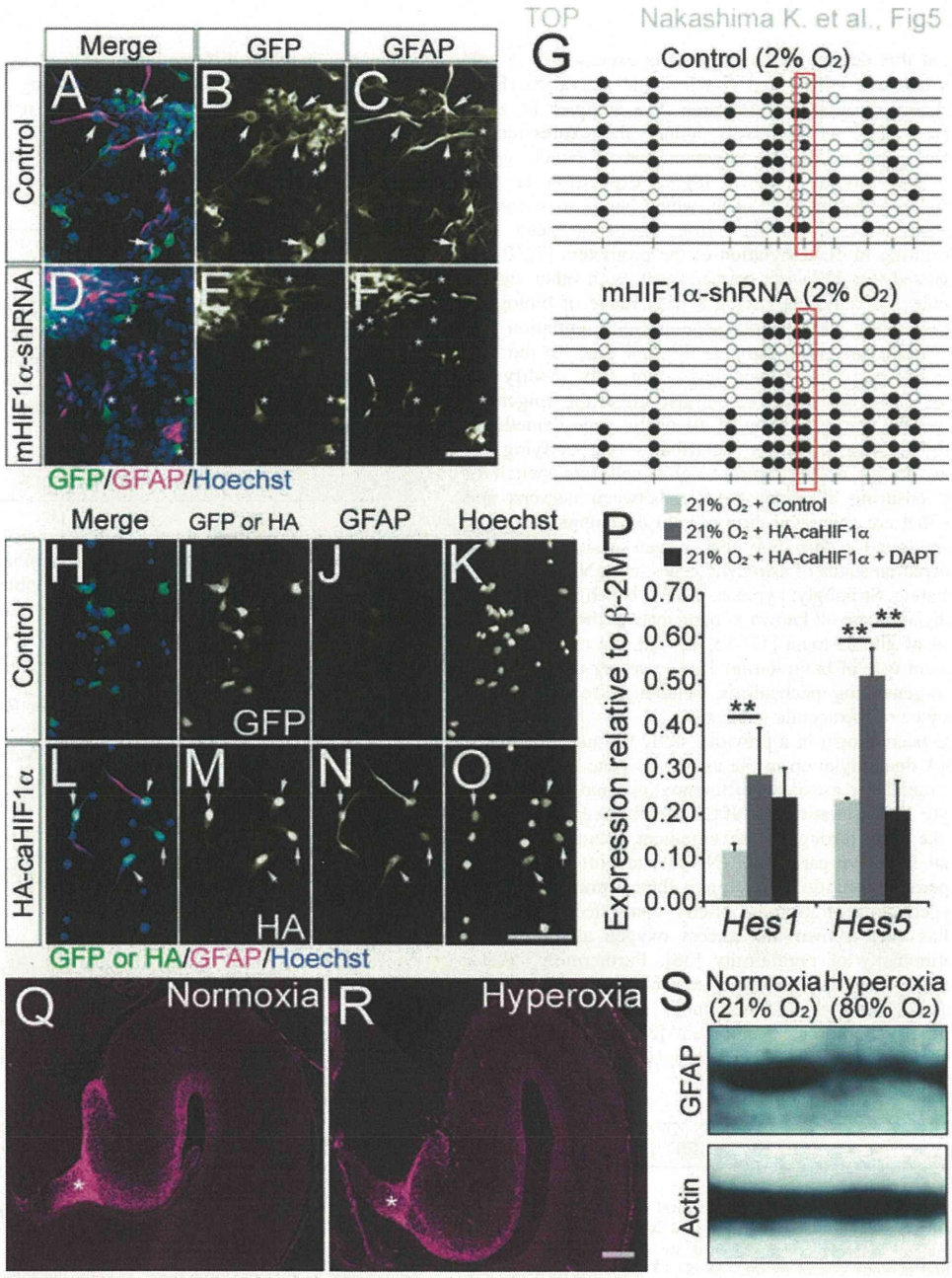

Figure 5. Astrogenic potential of neural precursor cells (NPCs) is regulated by HIF1α and oxygen levels. **(A–F):** E11.5 NPCs were infected with lentiviruses encoding GFP alone or GFP together with mHIF1α-shRNA, and cultured under 2% O_2 for 3 days followed by a 4-day leukemia inhibitory factor (LIF) stimulation. Virus-infected cells were identified by their GFP expression (green) and analyzed for GFAP expression (magenta) by immunocytochemistry. Hoechst, blue. GFP and GFAP double-positive cells (arrows) were observed in control virus-infected cells (A–C), whereas most of the mHIF1α-shRNA-expressing virus-infected cells were positive for GFP only (asterisks) (D–F). Bar = 50 μm. **(G):** The methylation status of the *gfap* promoter in 3-day-cultured virus-infected cells was examined by bisulfite sequencing. Demethylation in mHIF1α-shRNA-expressing virus-infected cells was inhibited. The signal transducer and activator of transcription 3-binding site is indicated by red rectangles. **(H–O):** Hydroxylation-mediated degradation-resistant constitutively active HIF1α (HA-caHIF1α) was introduced into E11.5 NPC by lentivirus infection, and the cells were cultured for 1 day followed by a 3-day LIF stimulation under 21% O_2. Precocious GFAP expression was observed in HA-caHIF1α-expressing virus-infected cells (arrows), even under 21% O_2 (L–O). Bar = 50 μm. **(P):** E11.5 NPCs were infected with control or HA-caHIF1α-expressing lentiviruses on the day after preparation and cultured in the presence of LIF for 3 days with or without DAPT under 21% O_2, and their RNAs were then subjected to quantitative polymerase chain reaction. *Hes1* and *Hes5* expression was normalized to that of β-2M. The expression of both of these genes was upregulated by HA-caHIF1α expression, and this effect was abolished by DAPT treatment. Statistical significance was evaluated by the Student's *t* test. **, $p < .01$. **(Q, R):** GFAP expression in E17.5 brain was reduced when pregnant mice were housed in a hyperoxic atmosphere (80% O_2) from E11.5 to E17.5. Brain sections are stained with anti-GFAP antibody (magenta). Hippocampal regions are shown as representatives. Asterisks, fimbria. Bar = 100 μm. **(S):** Whole brains of embryos from pregnant mice housed in normoxic (21% O_2) and hyperoxic (80% O_2) atmospheres were lysed and subjected to immunoblot to detect GFAP and β-actin (as loading control) expression. Abbreviations: β-2M, β-2 microglobulin; caHIF1α, constitutively active HIF1α; DAPT, *N*-[*N*-(3,5-difluorophenacetyl-L-alanyl)]-*S*-phenylglycine *t*-butyl ester); GFAP, glial fibrillary acidic protein; GFP, green fluorescent protein; HA, hemagglutinating; mHIF1α, mouse HIF1α; shRNA, short hairpin RNA.

suggest that this demethylation process is executed by a collaboration between HIF1α and Notch signal activation (Figs. 4, 5), probably through the formation of a complex between HIF1α and NICD, to effectively induce the expression of Notch-target genes [15]. The augmentation of Notch signal activation under hypoxia led to higher expression of *Nfia* (Supporting Information Fig. S4A), which has been shown to induce dissociation of DNMT1 from astrocytic gene promoters, resulting in demethylation of the promoters [7]. It has been suggested that HIFs act cooperatively with other signaling molecules, thereby influencing a wide range of biological processes including NPC maintenance and differentiation [11, 18-20]. Nevertheless, we report for the first time, to the best of our knowledge, that oxygen levels not only modify the behavior of transcription factors but also affect the epigenetic status of genes. The promotion of astrocytic gene demethylation by the hypoxic condition contributes to specifying the appropriate timing of the neural-to-glial cell fate switch of NPCs, by ensuring a proper balance between neurons and astrocytes that are generated during brain development.

We also found in this study that oxygen tension affects the DNA methylation status of astrocytic genes in mgNPCs via HIF-Notch signaling. Strikingly, hypoxia, HIF1α, Notch signaling and DNA methylation are all known to participate in the onset and/or progression of glioblastoma [12, 13, 15, 37], the most common and malignant type of brain tumor. Thus, a deeper understanding of glial cell-generating mechanisms, including astrocyte differentiation, may be of therapeutic interest.

As has been shown in a previous study [5] and the present work, DNA demethylation in the astrocytic gene promoters of NPCs is crucial for astrocyte differentiation, and the efficacy of astrocyte differentiation of NPCs is influenced by oxygen levels in the brain throughout development. Premature infants in neonatal intensive care units (NICUs) are often incubated under hyperoxic conditions to support their immature respiration. Oxygen concentration is strictly controlled in NICUs, since it has been shown that excess oxygen administration causes retinopathy of prematurity [38]. Furthermore, a few studies report other risks of hyperoxia to the central nervous system of extremely premature infants, including defects in mental and psychomotor development [39, 40]. The present study suggests that such effects may be attributable to an imbalance in NPC differentiation caused by a high level of oxygen in the incubator, and identifying their underlying mechanism in future work could provide new approaches for clinical applications that address developmental abnormalities in the nervous system, particularly in the context of neonatal intensive care.

Conclusion

We showed that local oxygen concentration can affect the fate of NPCs through an epigenetic mechanism. Unraveling how actual microenvironmental oxygen levels in the embryo influence epigenetic gene regulation in NPCs will provide new aspects for the study of NPC regulation.

Acknowledgments

We thank T. Kobayashi for the hyperoxic oxygen chamber, H. Harada, M. Hiraoka, T. Takizawa, M. Namihira, Y. Bessho, T. Matsui, Y. Nakahata, and K. Semi for valuable discussions and technical advice, I. Smith for editing the manuscript, and M. Tano for secretarial assistance. This work was supported by a Grant-in-Aid for Young Scientists (Start-up), Grant-in-Aid for Scientific Research on Innovative Area: Neural Diversity and Neocortical Organization, Grant-in-Aid for Research Program of Innovative Cell Biology by Innovative Technology and by the NAIST Global COE Program (Frontier Biosciences: Strategies for survival and adaptation in a changing global environment) from the Ministry of Education, Culture, Sports, Science and Technology of Japan; Health Sciences Research Grants from the Ministry of Health, Labor and Welfare, Japan. T.M. is currently affiliated with Biological Sciences, Gunma Kokusai Academy Secondary School, Ota, Gunma, Japan.

Disclosure of Potential Conflicts of Interest

The authors indicate no potential conflicts of interest.

References

1 Hirabayashi Y, Gotoh Y. Epigenetic control of neural precursor cell fate during development. Nat Rev Neurosci 2010;11:377–388.
2 Bonni A, Sun Y, Nadal-Vicens M et al. Regulation of gliogenesis in the central nervous system by the JAK-STAT signaling pathway. Science 1997;278:477–483.
3 Nakashima K, Wiese S, Yanagisawa M et al. Developmental requirement of gp130 signaling in neuronal survival and astrocyte differentiation. J Neurosci 1999;19:5429–5434.
4 Fan G, Martinowich K, Chin MH et al. DNA methylation controls the timing of astrogliogenesis through regulation of JAK-STAT signaling. Development 2005;132:3345–3356.
5 Takizawa T, Nakashima K, Namihira M et al. DNA methylation is a critical cell-intrinsic determinant of astrocyte differentiation in the fetal brain. Dev Cell 2001;1:749–758.
6 Pierfelice T, Alberi L, Gaiano N. Notch in the vertebrate nervous system: An old dog with new tricks. Neuron 2011;69:840–855.
7 Namihira M, Kohyama J, Semi K et al. Committed neuronal precursors confer astrocytic potential on residual neural precursor cells. Dev Cell 2009;16:245–255.
8 Slater TF. Free-radical mechanisms in tissue injury. Biochem J. 1984; 222:1–15.
9 Bruick RK, McKnight SL. A conserved family of prolyl-4-hydroxylases that modify HIF. Science 2001;294:1337–1340.
10 Sang N, Fang J, Srinivas V et al. Carboxyl-terminal transactivation activity of hypoxia-inducible factor 1 alpha is governed by a von Hippel-Lindau protein-independent, hydroxylation-regulated association with p300/CBP. Mol Cell Biol 2002;22:2984–2992.
11 Simon MC, Keith B. The role of oxygen availability in embryonic development and stem cell function. Nat Rev Mol Cell Biol 2008;9: 285–296.
12 Lofstedt T, Jogi A, Sigvardsson M et al. Induction of ID2 expression by hypoxia-inducible factor-1: A role in dedifferentiation of hypoxic neuroblastoma cells. J Biol Chem 2004;279:39223–39231.
13 Semenza G. Signal transduction to hypoxia-inducible factor 1. Biochem Pharmacol 2002;64:993–998.
14 Tomita S, Ueno M, Sakamoto M et al. Defective brain development in mice lacking the Hif-1alpha gene in neural cells. Mol Cell Biol 2003;23:6739–6749.
15 Gustafsson MV, Zheng X, Pereira T et al. Hypoxia requires notch signaling to maintain the undifferentiated cell state. Dev Cell 2005;9: 617–628.
16 Dunlop EA, Tee AR. Mammalian target of rapamycin complex 1: Signalling inputs, substrates and feedback mechanisms. Cell Signal 2009; 21:827–835.
17 Land SC, Tee AR. Hypoxia-inducible factor 1alpha is regulated by the mammalian target of rapamycin (mTOR) via an mTOR signaling motif. J Biol Chem 2007;282:20534–20543.
18 Jogi A, Ora I, Nilsson H et al. Hypoxia alters gene expression in human neuroblastoma cells toward an immature and neural crest-like phenotype. Proc Natl Acad Sci USA 2002;99:7021–7026.

19 Chen HL, Pistollato F, Hoeppner DJ et al. Oxygen tension regulates survival and fate of mouse central nervous system precursors at multiple levels. Stem Cells 2007;25:2291–2301.
20 Mohyeldin A, Garzon-Muvdi T, Quinones-Hinojosa A. Oxygen in stem cell biology: A critical component of the stem cell niche. Cell Stem Cell 2010;7:150–161.
21 Wright WE, Shay JW. Inexpensive low-oxygen incubators. Nat Protoc 2006;1:2088–2090.
22 Moeller BJ, Dreher MR, Rabbani ZN et al. Pleiotropic effects of HIF-1 blockade on tumor radiosensitivity. Cancer Cell 2005;8:99–110.
23 Zhou Z, Hong EJ, Cohen S et al. Brain-specific phosphorylation of MeCP2 regulates activity-dependent Bdnf transcription, dendritic growth, and spine maturation. Neuron 2006;52:255–269.
24 Lois-Caballe C, Baltimore D, Qin X-F. Method for expression of small antiviral RNA molecules within a cell. US Patent0 059 944 Al. 2003.
25 Mutoh T, Miyata T, Kashiwagi S et al. Dynamic behavior of individual cells in developing organotypic brain slices revealed by the photoconvertable protein Kaede. Exp Neurol 2006;200:430–437.
26 Papkovskii DB, Yaropolov AI, Savitskii AP et al. Fibre-optic oxygen sensor based on phosphorescence quenching. Biomed Sci 1991;2: 536–539.
27 Hatada I, Namihira M, Morita S et al. Astrocyte-specific genes are generally demethylated in neural precursor cells prior to astrocytic differentiation. PLoS One 2008;3:e3189.
28 Dunwoodie SL. The role of hypoxia in development of the Mammalian embryo. Dev Cell 2009;17:755–773.
29 Arteel GE, Thurman RG, Raleigh JA. Reductive metabolism of the hypoxia marker pimonidazole is regulated by oxygen tension independent of the pyridine nucleotide redox state. Eur J Biochem 1998: 253:743–750.
30 Raleigh JA, La Dine JK, Cline JM et al. An enzyme-linked immunosorbent assay for hypoxia marker binding in tumours. Br J Cancer 1994;69:66–71.
31 Iyer NV, Kotch LE, Agani F et al. Cellular and developmental control of O_2 homeostasis by hypoxia-inducible factor 1 alpha. Genes Dev 1998;12:149–162.
32 Jain S, Maltepe E, Lu MM et al. Expression of ARNT, ARNT2, HIF1 Alpha, HIF2 alpha and Ah receptor Mrnas in the developing mouse. Mech Dev 1998;73:117–123.
33 Kaelin WG Jr, Ratcliffe PJ. Oxygen sensing by metazoans: The central role of the HIF hydroxylase pathway. Mol Cell 2008;30:393–402.
34 Palmer LA, Semenza GL, Stoler MH et al. Hypoxia induces type II NOS gene expression in pulmonary artery endothelial cells via HIF-1. Am J Physiol 1998;274:L212–L219.
35 Roitbak T, Surviladze Z, Cunningham LA. Continuous expression of HIF-1alpha in neural stem/progenitor cells. Cell Mol Neurobiol 2011; 31:119–133.
36 Hirsila M, Koivunen P, Gunzler V et al. Characterization of the human prolyl 4-hydroxylases that modify the hypoxia-inducible factor. J Biol Chem 2003;278:30772–30780.
37 Martinez R, Esteller M. The DNA methylome of glioblastoma multiforme. Neurobiol Dis 2011;39:40–46.
38 Quinn GE, Dobson V. Outcome of prematurity and retinopathy of prematurity. Curr Opin Ophthalmol 1996;7:51–56.
39 Blackburn S. Environmental impact of the NICU on developmental outcomes. J Pediatr Nurs 1998;13:279–289.
40 Deulofeut R, Critz A, Adams-Chapman I et al. Avoiding hyperoxia in infants < or = 1250 g is associated with improved short- and long-term outcomes. J Perinatol 2006;26:700–705.

See www.StemCells.com for supporting information available online.

Neuroscience Research 72 (2012) 23–31

Contents lists available at SciVerse ScienceDirect

Neuroscience Research

journal homepage: www.elsevier.com/locate/neures

Induction of superficial cortical layer neurons from mouse embryonic stem cells by valproic acid

Berry Juliandi[a,b], Masahiko Abematsu[a,c], Tsukasa Sanosaka[a], Keita Tsujimura[a], Austin Smith[d,e], Kinichi Nakashima[a,*]

[a] Laboratory of Molecular Neuroscience, Graduate School of Biological Sciences, Nara Institute of Science and Technology, Ikoma, Nara 630-0192, Japan
[b] Department of Biology, Bogor Agricultural University (IPB), Bogor, Indonesia
[c] Department of Orthopaedic Surgery, Graduate School of Medical and Dental Sciences, Kagoshima University, Kagoshima, Japan
[d] Wellcome Trust Centre for Stem Cell Research, University of Cambridge, Cambridge, United Kingdom
[e] Department of Biochemistry, University of Cambridge, Cambridge, United Kingdom

ARTICLE INFO

Article history:
Received 17 August 2011
Received in revised form
13 September 2011
Accepted 29 September 2011
Available online 6 October 2011

Keywords:
Neurogenesis
Corticogenesis
mESCs
HDAC inhibitor
Valproic acid
Histone acetylation

ABSTRACT

Within the developing mammalian cortex, neural progenitors first generate deep-layer neurons and subsequently more superficial-layer neurons, in an inside-out manner. It has been reported recently that mouse embryonic stem cells (mESCs) can, to some extent, recapitulate cortical development *in vitro*, with the sequential appearance of neurogenesis markers resembling that in the developing cortex. However, mESCs can only recapitulate early corticogenesis; superficial-layer neurons, which are normally produced in later developmental periods *in vivo*, are under-represented. This failure of mESCs to reproduce later corticogenesis *in vitro* implies the existence of crucial factor(s) that are absent or uninduced in existing culture systems. Here we show that mESCs can give rise to superficial-layer neurons efficiently when treated with valproic acid (VPA), a histone deacetylase inhibitor. VPA treatment increased the production of Cux1-positive superficial-layer neurons, and decreased that of Ctip2-positive deep-layer neurons. These results shed new light on the mechanisms of later corticogenesis.

1. Introduction

The mammalian cerebral cortex displays a complex structure with a high diversity of neuronal subtypes (Molyneaux et al., 2007). Within this structure, approximately 80% of the neurons are pyramidal excitatory cells which are derived from radial glial progenitors in the ventricular zone (VZ), and are generated in a well defined spatio-temporal manner (Guillemot et al., 2006; Leone et al., 2008). The first neurons generated are Cajal-Retzius cells, which will reside in the most superficial cortical layer (layer I). Subsequent neurogenesis proceeds in an inside-out fashion, by producing deep-layer neurons (layers V and VI) and then progressively more superficial-layer neurons (layers II–IV).

We have devised an adherent monolayer culture of mouse embryonic stem cells (mESCs) for the efficient generation of neuroectodermal precursors and neural stem cells (Ying et al., 2003; Conti et al., 2005). This system reduces the limitation and complexity of neural induction that are characteristic of multicellular aggregation (Bain et al., 1995; Wiles and Johansson, 1999) and/or co-culture methods (Kawasaki et al., 2000), and permits direct observation and manipulation of the cells under study. Recently, a better understanding of cortical neurogenesis was attained using our monolayer culture system. Gaspard et al. (2008) showed that, in the presence of sonic hedgehog (Shh) inhibitor, mESCs generate cortical neurons in a sequential fashion similar to that observed in the developing cortex. Despite this breakthrough result, the experiment failed to completely recapitulate later aspects of cortical development. Gaspard et al. (2008) had better success in generating early-born or deep-layer neurons than in generating superficial-layer neurons. Earlier, Shen et al. (2006) also reported that fewer superficial-layer neurons than deep-layer neurons were generated when they cultured cortical neural stem cells isolated at different gestational time points. This inefficiency in reproducing later events of cortical neurogenesis *in vitro* implies the existence of crucial factors which are not present or induced in current experimental systems.

Epigenetic mechanisms such as DNA methylation and histone modification including acetylation are now known to be critical intrinsic programs that dictate fate specification and differentiation of stem cells. Histone acetylation and deacetylation are mediated by histone acetyltransferases (HATs) and histone deacetylases (HDACs), respectively. In general, an increase of histone acetylation

* Corresponding author. Tel.: +81 743 72 5471; fax: +81 743 72 5479.
E-mail address: kin@bs.naist.jp (K. Nakashima).

0168-0102/$ – see front matter © 2011 Elsevier Ireland Ltd and the Japan Neuroscience Society. All rights reserved.
doi:10.1016/j.neures.2011.09.012

by HATs causes the remodeling of chromatin from a tightly to a loosely packed configuration, leading to transcriptional activation. Conversely, a decrease of histone acetylation by HDACs results in a condensed chromatin structure and thus suppresses transcription (Juliandi et al., 2010). Inhibition of HDAC activity by valproic acid (VPA), a widely used anticonvulsant and mood-stabilizing drug, has been shown to drive mESCs to differentiate into the ectodermal lineage at the expense of mesodermal and endodermal lineages (Murabe et al., 2007). This ectodermal lineage differentiation is further biased in favor of neuronal rather than glial fates by the VPA treatment (Murabe et al., 2007). Prior to this finding in mESCs, we and others (Hsieh et al., 2004; Balasubramaniyan et al., 2006) had also found a similar tendency for neuronal over glial fate preference when we cultured neural progenitor cells (NPCs) in the presence of HDAC inhibitors such as VPA and trichostatin A. The types of neurons produced in these studies were not examined in detail, however, and the effects of HDAC inhibition on the differentiation of mESC-derived NPCs have not yet been studied.

Here we report that HDAC inhibition in mESC-derived NPCs treated with VPA resulted in a recapitulation of later stages of corticogenesis. VPA treatment increased the production of cut-like homeobox 1 (Cux1)-positive superficial-layer neurons and decreased that of B-cell leukemia/lymphoma 11B (Bcl11b; also called Ctip2)-positive deep-layer neurons. These results suggest an important role of histone acetylation for the specification of superficial-layer neurons in late corticogenesis.

2. Materials and methods

2.1. Maintenance of mESCs

The mESC line 46C (*Sox1*-GFP-IRES-pac knock-in) was routinely propagated without feeder cells as described previously (Ying et al., 2003; Conti et al., 2005). mESCs were grown at 37 °C in a 5% (v/v) CO_2 incubator in ESC medium (ESM) containing Glasgow Minimum Essential Medium (Invitrogen), supplemented with 10% (v/v) fetal bovine serum (Biowest), 1 mM sodium pyruvate (Invitrogen), 0.1 mM MEM non-essential amino acids (Invitrogen), 0.1 mM 2-mercaptoethanol (Sigma), and 1000 U/ml murine leukemia inhibitory factor (Millipore), on 0.1% (v/v) gelatin-coated (Sigma) 9-cm dishes (Nunc). Medium was changed every day, and when the cells reached 60–70% confluence they were passaged onto new dishes at a plating density of 1×10^6 cells per 9-cm dish.

2.2. Neural differentiation

mESCs were induced to differentiate to the neural lineage as described previously (Ying et al., 2003; Conti et al., 2005; Gaspard et al., 2008, 2009). In brief, mESCs were trypsinized, dissociated and plated on 0.1% (v/v) gelatin-coated (Sigma) dishes at a density of 0.3×10^6 cells per 9-cm dish (Nunc) in ESM. One day later, the medium was replaced with DDM, which is composed of DMEM/F12 (Invitrogen) supplemented with freshly prepared modified N2-supplement (Ying and Smith, 2003), 1 mM sodium pyruvate (Invitrogen), 0.1 mM MEM non-essential amino acids (Invitrogen), 0.1 mM 2-mercaptoethanol (Sigma), 0.5 mg/ml bovine serum albumin fraction V (Invitrogen), 1× GlutaMAX (Invitrogen) and 0.5× antibiotic–antimycotic (Invitrogen). This day was designated as differentiation day 0. Cyclopamine (Calbiochem) was added to a final concentration of 1 μM from differentiation day 2 to day 10. On differentiation day 10, the medium was replaced with DDM only (without cyclopamine). For selection of Sox1-expressing neural progenitor cells, from differentiation day 8 to day 10, puromycin (Sigma) was added to a final concentration of 0.5 μg/ml. The culture was maintained until differentiation day 12 and the medium was changed every 2 days during day 0 to day 12.

At differentiation day 12, mESC-derived NPCs were trypsinized, dissociated and plated on poly-L-lysine/laminin-coated (Sigma, Becton Dickinson) dishes at a density of 0.5×10^6 cells per 3.5-cm dish (Nunc) in N2/B27 medium, which consists of a 1:1 mixture of DDM (without sodium pyruvate and MEM non-essential amino acids) and Neurobasal/B27 medium (Neurobasal, 1× B27 supplement without vitamin A, 1× GlutaMAX and 0.5× antibiotic–antimycotic (all from Invitrogen)). Valproic acid (Sigma) was added one time to the culture medium to a final concentration of 0.5 mM at differentiation day 12 where appropriate. Culture was maintained until differentiation day 14 or 21, and the medium was changed every 2 days during day 12 to day 21.

2.3. Immunocytochemistry

Medium was removed and cells were washed with phosphate buffered saline (PBS) and then fixed with 4% paraformaldehyde in PBS for 15 min. After 3 washes with PBS, the cells were incubated for 1 h at room temperature (RT) in blocking solution (PBS containing 3% FBS and 0.1% Triton X-100). They were then incubated overnight at 4 °C with the appropriate primary antibodies. The following primary antibodies were used: chick anti-GFP (1:500, Aves Labs), rabbit anti-β-tubulin isotype III (Tuj1; 1:1000, Covance), mouse anti-nestin (1:250, Millipore), rabbit anti-Pax6 (1:500, Covance), mouse anti-Map2ab (1:1000, Sigma), rat anti-Ctip2 (1:1000, Abcam), mouse anti-reelin (1:1000, MBL), and rabbit anti-Cux1 (1:500, Santa Cruz). After 3 washes with PBS, the cells were incubated for 2 h at RT with the appropriate secondary antibodies. The following secondary antibodies were used: FITC-conjugated donkey anti-chick, Cy5-conjugated donkey anti-rabbit, Cy3-conjugated donkey anti-rabbit, Cy5-conjugated donkey anti-mouse, Cy3-conjugated donkey anti-mouse (all 1:500, Jackson ImmunoResearch), Alexa Fluor 488-conjugated donkey anti-mouse, Alexa Fluor 488-conjugated donkey anti-rabbit, and Alexa Fluor 488-conjugated donkey anti-rat (all 1:500, Invitrogen). After 3 washes with PBS, nuclei were stained for 15 min at RT with Hoechst 33258 (Nacalai Tesque). Cells were washed with PBS, mounted on cover slips with Immu-Mount (Thermo Scientific), and examined and photographed using a fluorescence microscope (Axiovert 200M, Zeiss) equipped with a camera and appropriate epifluorescence filters.

3. Results

3.1. 46C mESCs differentiate into the neuroectodermal lineage under Shh inhibition

We used 46C mESCs, one of whose characteristic features is the replacement of the *Sox1* open reading frame with that encoding green fluorescent protein (GFP) (Ying et al., 2003). Since *Sox1* is the earliest known neuroectodermal marker in the mouse embryo (Pevny et al., 1998; Wood and Episkopou, 1999), we could follow neural commitment of 46C mESCs in culture by monitoring their GFP expression.

46C mESCs can differentiate efficiently into the neural lineage in feeder-free adherent monolayer culture supplemented with serum-free medium (Ying et al., 2003; Conti et al., 2005; Abranches et al., 2009). *Sox1*-GFP-expressing NPCs can be detected from differentiation day 2, and composed more than 75% of the total cell population at differentiation day 4 in N2/B27 medium (Ying et al., 2003). To assess the neural commitment of 46C mESCs in the adherent monolayer culture system proposed by Gaspard et al. (2008), we cultured these cells at low density in a chemically defined

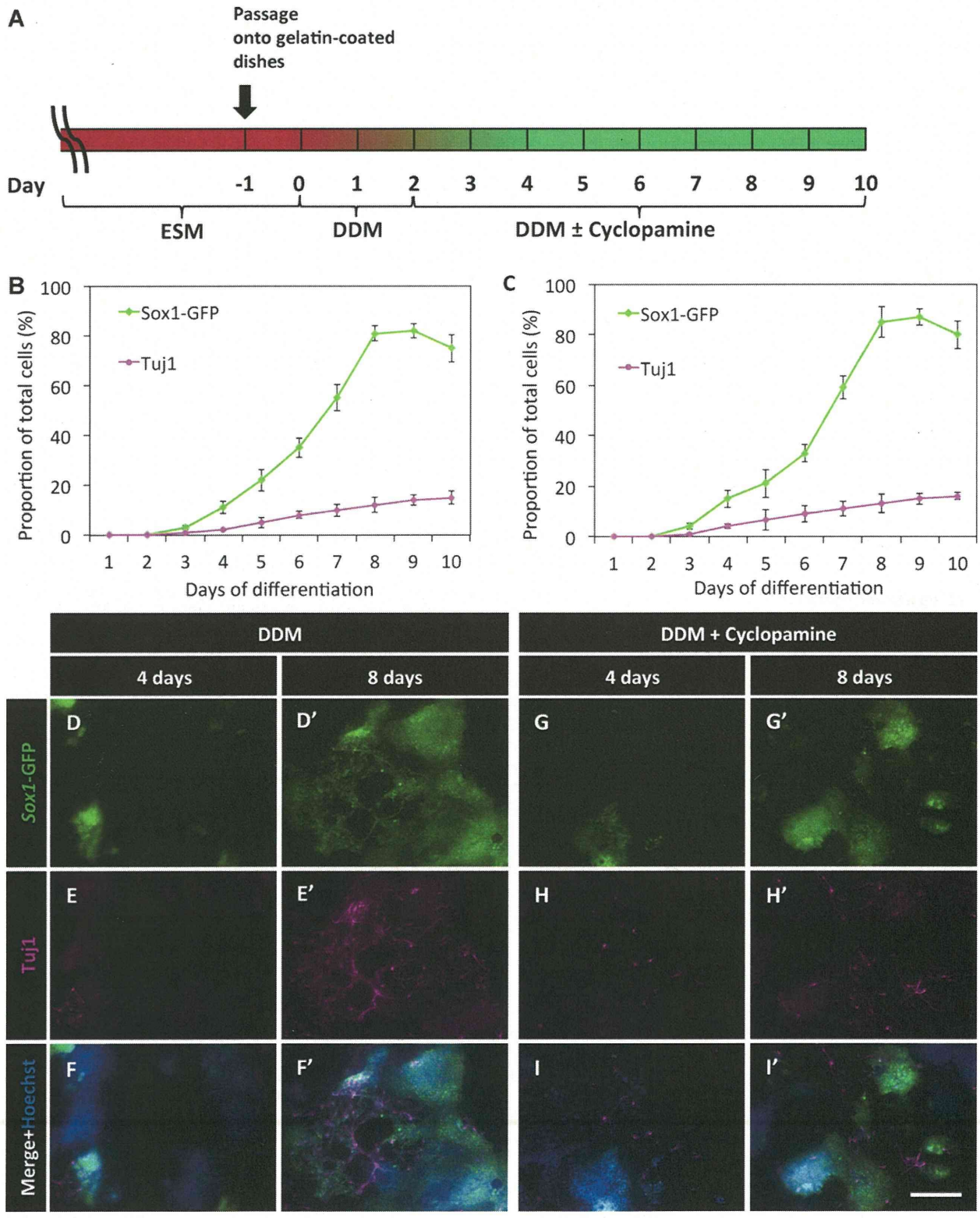

Fig. 1. 46C mESCs differentiate to the neuroectodermal lineage. (A) Timeline of the neural induction protocol using chemically defined default medium (DDM). mESCs were routinely propagated and then passaged to gelatin-coated dishes in embryonic stem cell medium (ESM) 1 day before neural induction (day −1). The next day (day 0), the medium was changed to DDM, and cyclopamine was added where appropriate from differentiation day 2 to day 10. The proportions of *Sox1*-GFP+ NPCs and Tuj1+ neurons did not differ in DDM (B) and in DDM with cyclopamine (C) during the culture period. Data are mean ± SD from at least three independent experiments. (D–I) Representative immunostaining images from differentiation day 4 and day 8 of *Sox1*-GFP-expressing (green in D, D′, G, and G′) and Tuj1-expressing (magenta in E, E′, H, and H′) cells, used for the quantitative data shown in B and C. Merged images with Hoechst (blue in F, F′, I, and I′) are also shown. Scale bar is 100 μm. (For interpretation of the references to color in this figure legend, the reader is referred to the web version of the article.)

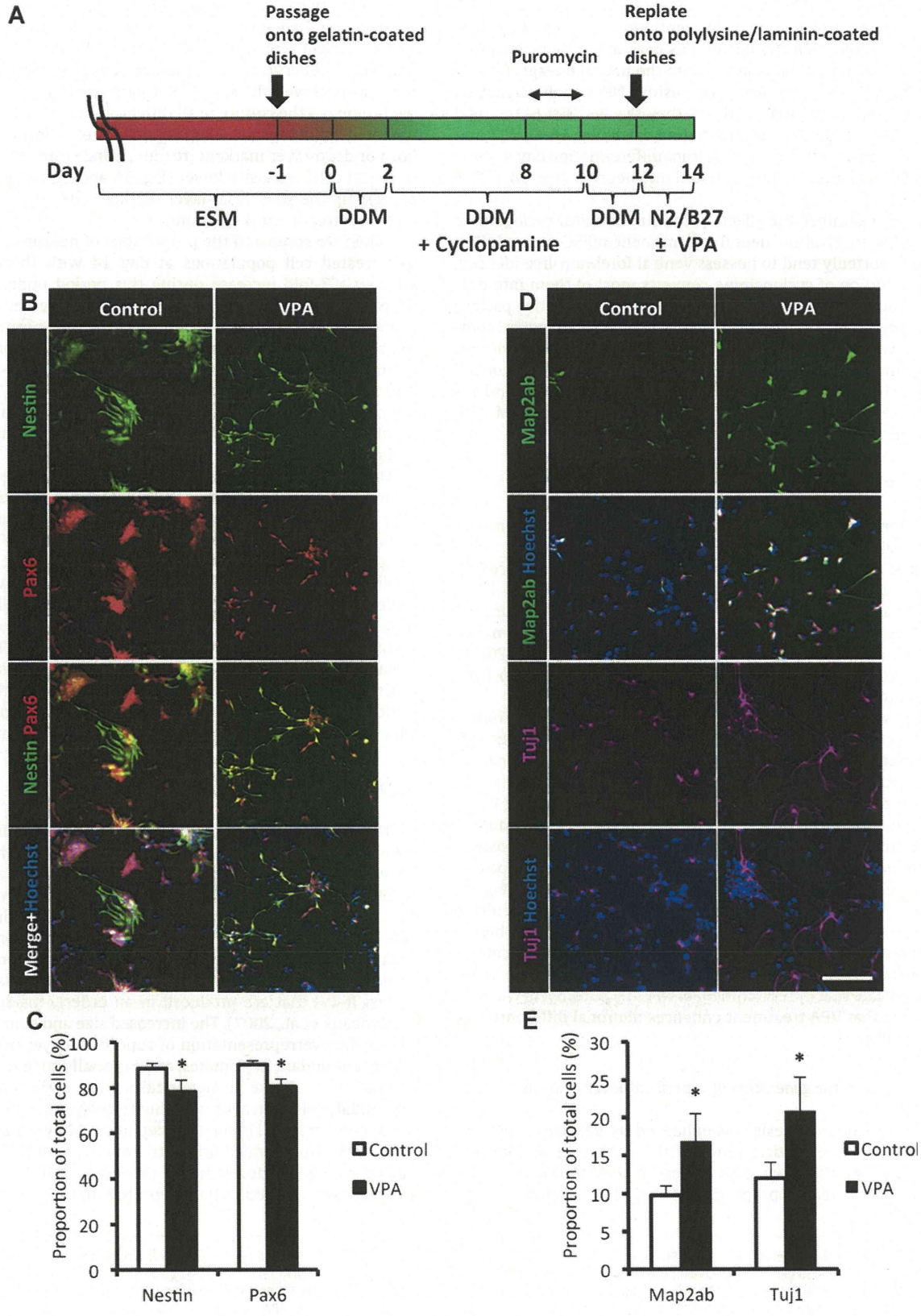
A
Passage
onto gelatin-coated
dishes
Puromycin
Replate
onto polylysine/laminin-coated
dishes
Day
-1
0
2
8
10
12
14
ESM
DDM
DDM
+ Cyclopamine
DDM
N2/B27
± VPA
B
Control
VPA
Nestin
Pax6
Nestin Pax6
Merge+Hoechst
D
Control
VPA
Map2ab
Map2ab Hoechst
Tuj1
Tuj1 Hoechst
C
Proportion of total cells (%)
100
80
60
40
20
0
*
*
Nestin
Pax6
Control
VPA
E
Proportion of total cells (%)
30
25
20
15
10
5
0
*
*
Map2ab
Tuj1
Control
VPA

default medium (DDM) for 10 days (Fig. 1A). We monitored *Sox1*-GFP expression and neuronal differentiation (as judged by Tuj1 immunostaining) each day during this period. We found that 46C mESCs differentiated more slowly into the neural lineage in DDM than in N2/B27. Although *Sox1*-GFP-positive NPCs could already be observed from differentiation day 3, they reached 80% of the total cell population only after differentiation day 8 (Fig. 1B, D, D′, F and F′). We also observed that starting from differentiation day 4, some of the NPCs had already differentiated into neurons (Fig. 1B, E, E′, F and F′).

We next examined the effects of the Shh inhibitor cyclopamine on 46C mESC survival and neural commitment. mESC-derived NPCs in DDM reportedly tend to possess ventral forebrain-like identity, and the addition of cyclopamine converts most of them into dorsal forebrain-like cells without affecting their proliferative pattern (Gaspard et al., 2008). We observed a similar pattern of neural commitment when we cultured 46C mESCs in DDM with or without cyclopamine, and found no significant difference in terms of cell survival (Fig. 1C, G–I and G′–I′). Thus, we conclude that 46C mESCs can survive and differentiate into the neural lineage in DDM with cyclopamine.

3.2. VPA enhances neurogenesis of 46C mESC-derived NPCs

Another advantage of using 46C mESCs is the existence of an internal ribosome entry site (IRES)-linked puromycin resistance gene which was also knocked-in together with GFP-encoding sequence to replace the *Sox1* gene's open reading frame (Ying et al., 2003). Hence, we can enrich the resulting NPCs by addition of puromycin to the medium. Because we found that the majority of 46C mESCs (>80%) had already differentiated into NPCs by differentiation day 8 (Fig. 1B and C), we added puromycin from differentiation day 8 to day 10 for our subsequent analysis.

Next, we examined the differentiation potential of enriched NPCs which were derived from 46C mESCs. We adopted the differentiation protocol of Gaspard et al. (2008, 2009) for making cortical neurons (Figs. 2A and 3A). At differentiation day 14 (Fig. 2A), we found that more than 80% of the cells were nestin- and Pax6-positive, indicating that they were mostly still NPCs (Fig. 2B and C). VPA treatment for 2 days reduced the proportion of cells positive for both markers (Fig. 2B and C). This reduction was accompanied by an increase of Map2ab- and Tuj1-positive neuronal cells (Fig. 2D and E). We then conducted the same analysis for a longer culture period, up to differentiation day 21 (Fig. 3A). We still found higher proportion of neuronal marker-positive (Map2ab+, Tuj1+) cells in the VPA-treated dishes compared with control (Fig. 3B and C). These results indicate that the enrichment of NPCs by puromycin was successful and that VPA treatment enhances neuronal differentiation of these NPCs.

3.3. VPA induces the generation of superficial-layer neurons

Given that neurogenesis was enhanced by VPA treatment, we then looked at the cortical types of these neurons at differentiation day 14 (after two days exposure to VPA; Fig. 2A). We first found a decreased proportion of early born and deep-layer neuron markers. The proportions of reelin- and Ctip2-positive cells among Tuj1-positive cells were significantly decreased by VPA treatment (Fig. 4A and C). Next, we found an increased proportion of superficial-layer marker (Cux1)-positive cells among Map2ab-positive cells after VPA treatment (Fig. 4B and D). When we prolonged the culture until differentiation day 21 (Fig. 3A), we obtained similar results. The proportions of cells positive for early born or deep-layer markers (reelin+, Ctip2+) among Tuj1-positive neuronal cells were still lower (Fig. 5A and C), while that for cells expressing the superficial-layer marker (Cux1+) was also higher, after VPA treatment (Fig. 5B and D).

When we compared the proportions of neurons in control and VPA-treated cell populations at day 14 with those at day 21, we saw a 3-fold increase during this period under both conditions (Figs. 2E and 3C). In control cells, we observed an increased proportion of Ctip2-positive cells among Tuj1-positive cells during this period (Figs. 4C and 5C). In contrast, the proportions of reelin- or Cux1-positive cells among neuronal marker-positive cells remained unchanged (Figs. 4C and D and 5C and D). These results indicate that in control cells, the majority of neurons produced during this period were Ctip2-positive, even though some of the NPCs still generated reelin- and Cux1-positive neurons.

On the other hand, the proportion of cells positive for the cortical markers we tested among neuronal marker-positive cells after VPA treatment did not change during the extended culture period (Figs. 4C and D and 5C and D). This indicates that VPA enhanced the production of Cux1-positive neurons only while it was being applied to the culture (differentiation day 12 to day 14). Nevertheless, the production of Ctip2-positive neurons in VPA treatment diminished compared to that in control cells during the extended culture period. These results suggest that transient VPA treatment enhances the temporal progression of some deep-layer-producing NPCs into superficial-layer-producing types during the treatment period, whereafter the residual NPCs retain this temporal progression even when VPA has been withdrawn from the culture.

4. Discussion

The brains of mammals differ in many aspects from those of other vertebrates. Most striking among the features that mammals have acquired during evolution are the increased size and complexity of the cerebral cortex, the largest brain structure where many of the higher cognitive functions reside (Finlay and Darlington, 1995; Hill and Walsh, 2005). The mammalian cerebral cortex is highly organized, with a six-layered structure that contains early-born or deep-layer (layers I, V and VI) and superficial-layer neurons (layers II–IV) that are produced in an orderly inside-out fashion (Molyneaux et al., 2007). The increased size and complexity partly reflect the overrepresentation of superficial-layer neurons, which are very abundant in primates, and especially so in human (Marin-Padilla, 1992). These cortical neurons are mainly of two types: pyramidal projection neurons, which mostly originate from NPCs of the dorsolateral wall of the telencephalon (Molyneaux et al., 2007), and interneurons, which originate from the ventral telencephalon during embryonic development (Wonders and Anderson, 2006). Although several studies have reported that ESCs can recapitulate

Fig. 2. VPA enhances neurogenesis of 46C mESC-derived NPCs. (A) Timeline of the corticogenesis protocol used for early differentiation analysis. mESCs were routinely propagated and passaged to gelatin-coated dishes in embryonic stem cells medium (ESM) 1 day before neural induction (day −1). The next day (day 0), medium was changed to chemically defined default medium (DDM) and cyclopamine was added from differentiation day 2 to day 10. At differentiation day 12, mESC-derived NPCs were replated to polylysine/laminin-coated dishes in N2/B27 (1:1 mixture of DDM and Neurobasal + B27). Valproic acid (VPA) was added where appropriate at differentiation day 12 and cells were harvested at differentiation day 14. (B–E) Representative immunostaining images from differentiation day 14 of nestin- and Pax6-expressing (green and red, respectively, in B), or Map2ab- and Tuj1-expressing (green and magenta, respectively, in D) cells and their quantification (C and E). Merged images with and without Hoechst (blue in B and D) are also shown. Tuj1 images in D were derived from the triple immunostaining data of Fig. 4A. Data are mean ± SD from at least three independent experiments. *$P < 0.05$ (Student's *t*-test). Scale bar is 100 μm. (For interpretation of the references to color in this figure legend, the reader is referred to the web version of the article.)

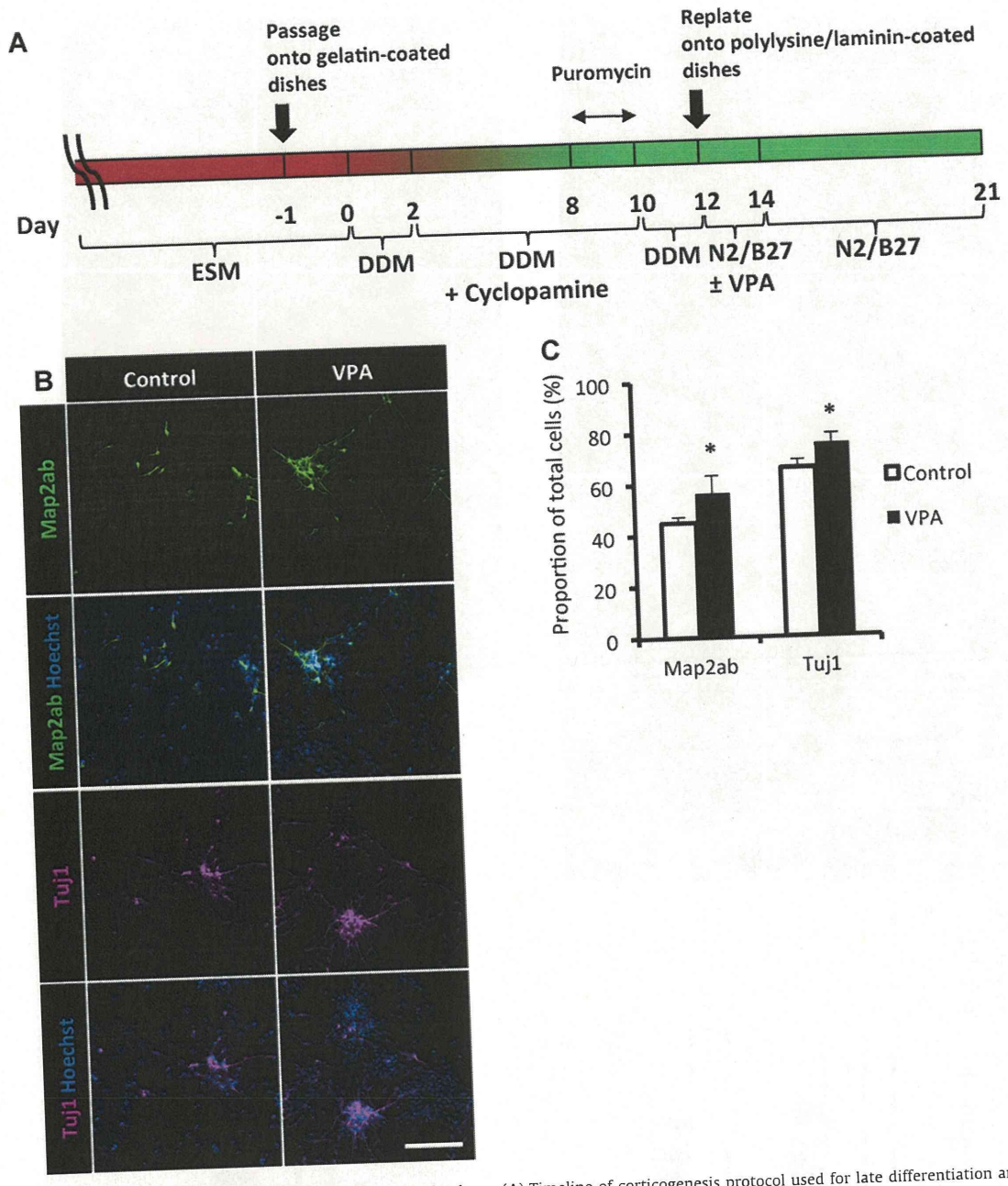

Fig. 3. Increased neurogenesis by VPA is observed even in prolonged culture. (A) Timeline of corticogenesis protocol used for late differentiation analysis. mESCs were routinely propagated and passaged to gelatin-coated dishes in embryonic stem cells medium (ESM) 1 day before neural induction (day −1). The next day (day 0), medium was changed to chemically defined default medium (DDM) and cyclopamine was added from differentiation day 2 to day 10. At differentiation day 12, mESC-derived NPCs were replated to polylysine/laminin-coated dishes in N2/B27 (1:1 mixture of DDM and Neurobasal + B27). Valproic acid (VPA) was added where appropriate at differentiation day 12 and cells were harvested at differentiation day 21. (B) Representative immunostaining images from differentiation day 21 of Map2ab- and Tuj1-expressing (green and magenta, respectively) cells. Merged images with Hoechst (blue) are also shown. Map2ab and Tuj1 images were derived from double- and triple-immunostaining data of Fig. 5A and B, respectively. (C) Quantification of neuronal marker-positive cells found in B. Data are mean ± SD from at least three independent experiments. $^*P < 0.05$ (Student's *t*-test). Scale bar is 100 μm. (For interpretation of the references to color in this figure legend, the reader is referred to the web version of the article.)

certain aspects of cortical neurogenesis *in vitro* (Eiraku et al., 2008; Gaspard et al., 2008), the generation of superficial-layer neurons in those studies was very limited.

In the present study, we have demonstrated that transient HDAC inhibition by VPA in 46C mESC-derived NPCs enhances their neuronal differentiation (Fig. 2D and E). This has been reported previously in several studies using different types of NPCs (Hsieh et al., 2004; Murabe et al., 2007; Yu et al., 2009). Using an mESC culture system that can specifically produce and recapitulate the generation of cortical-layer neurons (Gaspard et al., 2008, 2009), we further showed that the increasing neuronal population after VPA treatment includes a higher proportion of superficial-layer neurons (Cux1+) (Fig. 4B and D), accompanied by a decreasing proportion of early-born or deep-layer neurons (reelin+, Ctip2+) (Fig. 4A and C). Therefore, it is conceivable that VPA enhances the temporal progression of some of deep-layer-producing NPCs into superficial-layer-producing NPCs during the time when VPA was being supplied to the culture. The residual NPCs retained this temporal progression even when VPA was withdrawn from the culture, because we still observed the same proportion of all cortical

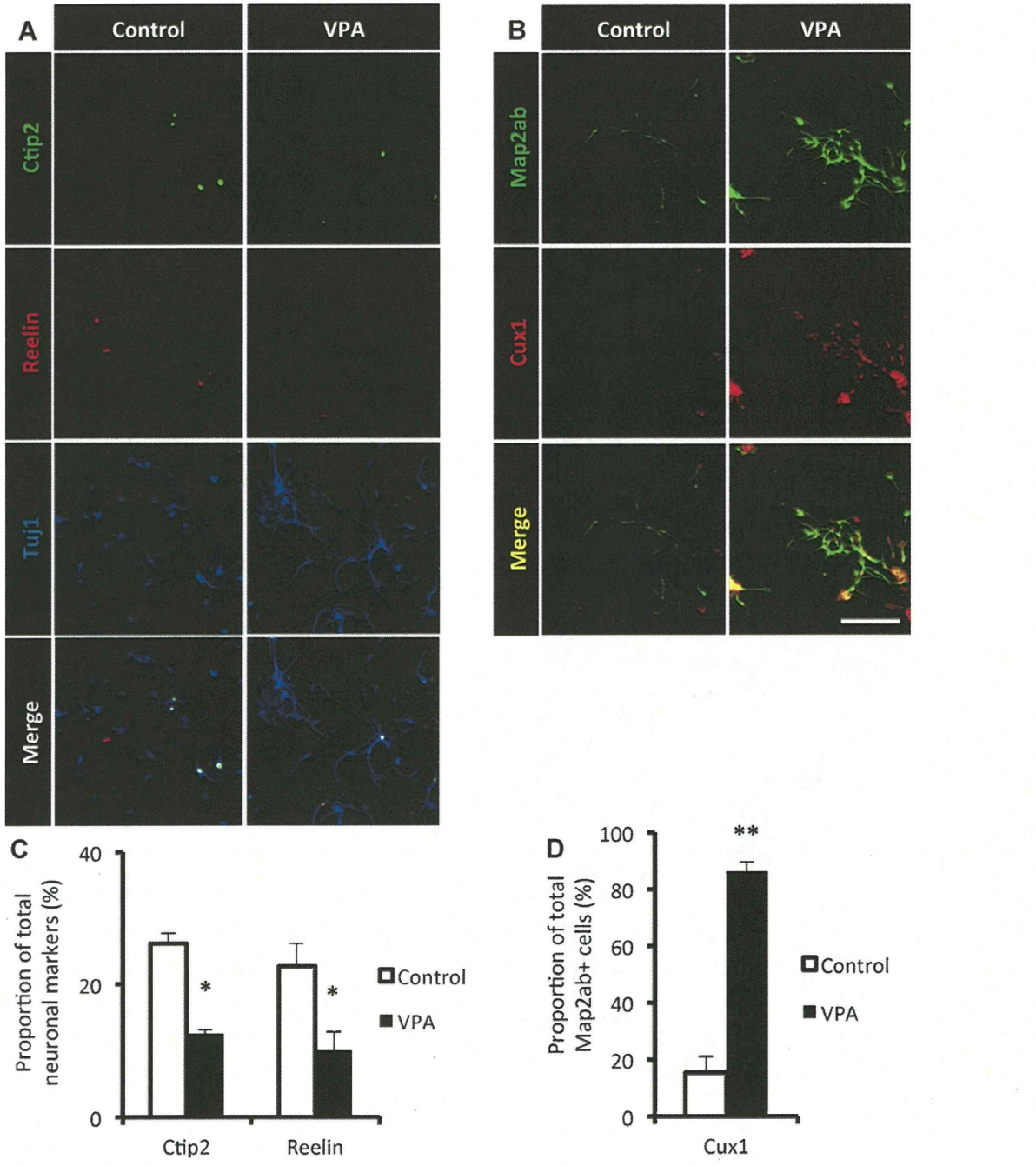

Fig. 4. VPA induces the production of superficial-layer neurons. (A and B) Representative immunostaining images from differentiation day 14, as in Fig. 2A, for Ctip2-, reelin- and Tuj1-expressing (green, red, and blue, respectively, in A), and Map2ab- and Cux1-expressing (green and red, respectively, in B) cells. Merged images are also shown. Hoechst staining can be found in Fig. 2D. Quantification of cortical layer marker-positive cells among neuronal marker-expressing cells for early-born or deep-layer (C) and superficial-layer neurons (D). Data are mean ± SD from at least three independent experiments. $^{*}P < 0.05$, $^{**}P < 0.001$ (Student's *t*-test). Scale bar is 100 μm. (For interpretation of the references to color in this figure legend, the reader is referred to the web version of the article.)

markers even at differentiation day 21, 7 days after VPA treatment was terminated (Fig. 5A–D).

Elucidating the mechanisms that lead to the enhanced progression of NPCs from producing deep-layer neurons to producing superficial-layer neurons after transient VPA treatment is an important challenge for future study. It has been proposed that the zinc-finger transcription factor *Fezf2*, which acts upstream of *Ctip2*, plays an important role in the specification of deep-layer neurons (Chen et al., 2008; Leone et al., 2008). VPA might repress *Fezf2* directly or indirectly in our culture system, which could in turn decrease the generation of deep-layer neurons and release the inhibition of upper-layer neuron production. This scenario is plausible, since VPA treatment of mouse embryos reduces levels of *Fezf2* mRNA in the forebrain (B.J. and K.N., unpublished data), and since there was an increase of Tbr1-positive cells in our culture after VPA treatment (data not shown). It has been reported recently that Tbr1 can act as a direct transcriptional repressor for *Fezf2* (Han et al., 2011).

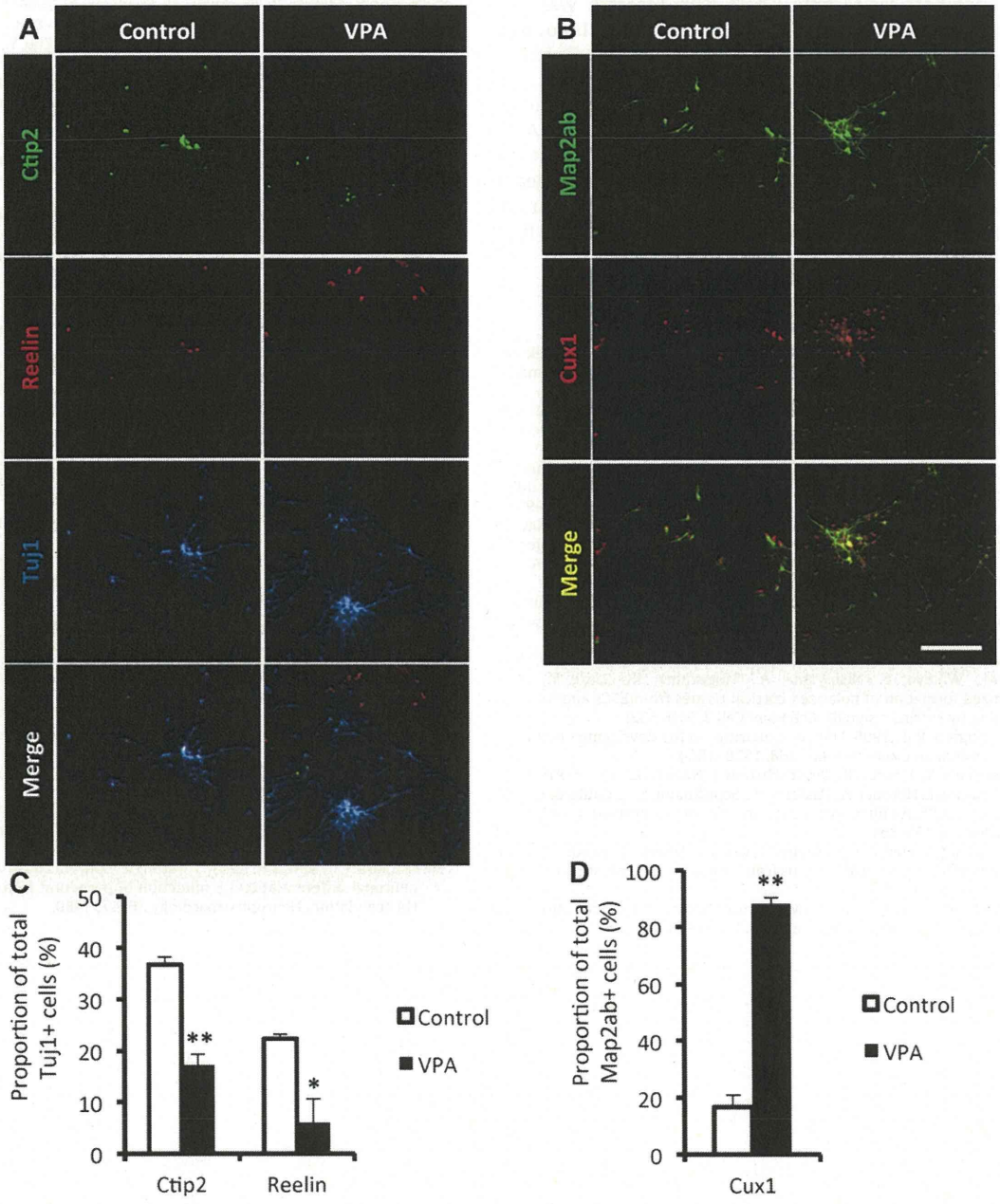

Fig. 5. Increased generation of superficial-layer neurons by VPA is observed even in prolonged culture. (A and B) Representative immunostaining images from differentiation day 21, as in Fig. 3A, for Ctip2-, reelin- and Tuj1-expressing (green, red, and blue, respectively, in A), and Map2ab- and Cux1-expressing (green and red, respectively, in B) cells. Merged images are also shown. Hoechst staining can be found in Fig. 3B. Quantification of cortical layer marker-positive cells among neuronal marker-expressing cells for early-born or deep-layer (C) and superficial-layer neurons (D). Data are mean ± SD from at least three independent experiments. $^{*}P < 0.05$, $^{**}P < 0.001$ (Student's *t*-test). Scale bar is 100 μm. (For interpretation of the references to color in this figure legend, the reader is referred to the web version of the article.)

Our results suggest that histone acetylation plays important roles in the production of superficial-layer neurons in an adherent monolayer system. Similar efficient production of superficial-layer neurons from mESCs was also recently reported in a study of modified embryoid body (EB) formation (Eiraku et al., 2008). It is tempting to hypothesize that in the EB, high levels of histone acetylation occur and persist until late differentiation to help ensure the generation of superficial layer neurons. Nevertheless, generation of cortical neurons from human (h)ESCs using the same EB method was skewed toward deep-layer identity (Eiraku et al., 2008), and both mESCs and hESCs failed to recapitulate the same inside-out pattern of cortical neurogenesis observed in the developing cortex (Au and Fishell, 2008; Gaspard and Vanderhaeghen, 2010). It will be of interest to explore the effects of increasing histone acetylation by VPA treatment on the production of superficial-layer neurons in hESCs, and whether histone acetylation plays a role in the inside-out mode of cortical neurogenesis.

Acknowledgments

We thank Y. Bessho, T. Matsui, Y. Nakahata, J. Kohyama, T. Takizawa and M. Namihira for valuable discussions. We also thank I. Smith for critical reading of the manuscript. We are very grateful to M. Tano for her excellent secretarial assistance and other

laboratory members for technical help. This research was supported in part by Grant-in-Aid for Scientific Research on Innovative Area: NAIST Global COE Program (Frontier Biosciences: Strategies for survival and adaptation in a changing global environment) from the Ministry of Education, Culture, Sports, Science and Technology of Japan; Grant-in-Aid for Scientific Research on Innovative Area: Neural Diversity and Neocortical Organization from the Ministry of Education, Culture, Sports, Science and Technology of Japan; Health Sciences Research Grants from the Ministry of Health, Labour and Welfare, Japan; and Research Fellowships for Young Scientists from the Japan Society for the Promotion of Science.

References

Abranches, E., Silva, M., Pradier, L., Schulz, H., Hummel, O., Henrique, D., Bekman, E., 2009. Neural differentiation of embryonic stem cells *in vitro*: a road map to neurogenesis in the embryo. PLoS ONE 4, e6286.

Au, E., Fishell, G., 2008. Cortex shatters the glass ceiling. Cell Stem Cell 3, 472–474.

Bain, G., Kitchens, D., Yao, M., Huettner, J.E., Gottlieb, D.I., 1995. Embryonic stem cells express neuronal properties *in vitro*. Dev. Biol. 168, 342–357.

Balasubramaniyan, V., Boddeke, E., Bakels, R., Küst, B., Kooistra, S., Veneman, A., Copray, S., 2006. Effects of histone deacetylation inhibition on neuronal differentiation of embryonic mouse neural stem cells. Neuroscience 143, 939–951.

Chen, B., Wang, S.S., Hattox, A.M., Rayburn, H., Nelson, S.B., McConnell, S.K., 2008. The Fezf2-Ctip2 genetic pathway regulates the fate choice of subcortical projection neurons in the developing cerebral cortex. Proc. Natl. Acad. Sci. U. S. A. 105, 11382–11387.

Conti, L., Pollard, S.M., Gorba, T., Reitano, E., Toselli, M., Biella, G., Sun, Y., Sanzone, S., Ying, Q.L., Cattaneo, E., Smith, A., 2005. Niche-independent symmetrical self-renewal of a mammalian tissue stem cell. PLoS Biol. 3, e283.

Eiraku, M., Watanabe, K., Matsuo-Takasaki, M., Kawada, M., Yonemura, S., Matsumura, M., Wataya, T., Nishiyama, A., Muguruma, K., Sasai, Y., 2008. Self-organized formation of polarized cortical tissues from ESCs and its active manipulation by extrinsic signals. Cell Stem Cell 3, 519–532.

Finlay, B.L., Darlington, R.B., 1995. Linked regularities in the development and evolution of mammalian brains. Science 268, 1578–1584.

Gaspard, N., Bouschet, T., Hourez, R., Dimidschstein, J., Naeije, G., van den Ameele, J., Espuny-Camacho, I., Herpoel, A., Passante, L., Schiffmann, S.N., Gaillard, A., Vanderhaeghen, P., 2008. An intrinsic mechanism of corticogenesis from embryonic stem cells. Nature 455, 351–357.

Gaspard, N., Bouschet, T., Herpoel, A., Naeije, G., van den Ameele, J., Vanderhaeghen, P., 2009. Generation of cortical neurons from mouse embryonic stem cells. Nat. Protoc. 4, 1454–1463.

Gaspard, N., Vanderhaeghen, P., 2010. Mechanisms of neural specification from embryonic stem cells. Curr. Opin. Neurobiol. 20, 37–43.

Guillemot, F., Molnár, Z., Tarabykin, V., Stoykova, A., 2006. Molecular mechanisms of cortical differentiation. Eur. J. Neurosci. 23, 857–868.

Han, W., Kwan, K.Y., Shim, S., Lam, M.M., Shin, Y., Xu, X., Zhu, Y., Li, M., Sestan, N., 2011. TBR1 directly represses Fezf2 to control the laminar origin and development of the corticospinal tract. Proc. Natl. Acad. Sci. U. S. A. 108, 3041–3046.

Hill, R.S., Walsh, C.A., 2005. Molecular insights into human brain evolution. Nature 437, 64–67.

Hsieh, J., Nakashima, K., Kuwabara, T., Mejia, E., Gage, F.H., 2004. Histone deacetylase inhibition-mediated neuronal differentiation of multipotent adult neural progenitor cells. Proc. Natl. Acad. Sci. U. S. A. 101, 16659–16664.

Juliandi, B., Abematsu, M., Nakashima, K., 2010. Chromatin remodeling in neural stem cell differentiation. Curr. Opin. Neurobiol. 20, 408–415.

Kawasaki, H., Mizuseki, K., Nishikawa, S., Kaneko, S., Kuwana, Y., Nakanishi, S., Nishikawa, S.I., Sasai, Y., 2000. Induction of midbrain dopaminergic neurons from ES cells by stromal cell-derived inducing activity. Neuron 28, 31–40.

Leone, D.P., Srinivasan, K., Chen, B., Alcamo, E., McConnell, S.K., 2008. The determination of projection neuron identity in the developing cerebral cortex. Curr. Opin. Neurobiol. 18, 28–35.

Marin-Padilla, M., 1992. Ontogenesis of the pyramidal cell of the mammalian neocortex and developmental cytoarchitectonics: a unifying theory. J. Comp. Neurol. 321, 223–240.

Molyneaux, B.J., Arlotta, P., Menezes, J.R.L., Macklis, J.D., 2007. Neuronal subtype specification in the cerebral cortex. Nat. Rev. Neurosci. 8, 427–437.

Murabe, M., Yamauchi, J., Fujiwara, Y., Hiroyama, M., Sanbe, A., Tanoue, A., 2007. A novel embryotoxic estimation method of VPA using ES cells differentiation system. Biochem. Biophys. Res. Commun. 352, 164–169.

Pevny, L.H., Sockanathan, S., Placzek, M., Lovell-Badge, R., 1998. A role for SOX1 in neural determination. Development 125, 1967–1978.

Shen, Q., Wang, Y., Dimos, J.T., Fasano, C.A., Phoenix, T.N., Lemischka, I.R., Ivanova, N.B., Stifani, S., Morrisey, E.E., Temple, S., 2006. The timing of cortical neurogenesis is encoded within lineages of individual progenitor cells. Nat. Neurosci. 6, 743–751.

Wiles, M.V., Johansson, B.M., 1999. Embryonic stem cell development in a chemically defined medium. Exp. Cell Res. 247, 241–248.

Wonders, C.P., Anderson, S.A., 2006. The origin and specification of cortical interneurons. Nat. Rev. Neurosci. 7, 687–696.

Wood, H.B., Episkopou, V., 1999. Comparative expression of the mouse Sox1, Sox2 and Sox3 genes from pre-gastrulation to early somite stages. Mech. Dev. 86, 197–201.

Ying, Q.L., Smith, A.G., 2003. Defined conditions for neural commitment and differentiation. Methods Enzymol. 365, 327–341.

Ying, Q.L., Stavridis, M., Griffiths, D., Li, M., Smith, A., 2003. Conversion of embryonic stem cells into neuroectodermal precursors in adherent monoculture. Nat. Biotechnol. 21, 183–186.

Yu, I.T., Park, J.Y., Kim, S.H., Lee, J.S., Kim, Y.S., Son, H., 2009. Valproic acid promotes neuronal differentiation by induction of proneural factors in association with H4 acetylation. Neuropharmacology 56, 473–480.

Journal of Pathology
J Pathol 2011; **224:** 169–179
Published online in Wiley Online Library
(wileyonlinelibrary.com) DOI: 10.1002/path.2880

ORIGINAL PAPER

Role of GLI2 in the growth of human osteosarcoma

Hiroko Nagao,[1] Kosei Ijiri,[1] Masataka Hirotsu,[1] Yasuhiro Ishidou,[2] Takuya Yamamoto,[1] Satoshi Nagano,[1] Takumi Takizawa,[3] Kinichi Nakashima,[3] Setsuro Komiya[1] and Takao Setoguchi[1]*

[1] *Department of Orthopaedic Surgery, Graduate School of Medical and Dental Sciences, Kagoshima University, Japan*
[2] *Department of Medical Joint Materials, Graduate School of Medical and Dental Sciences, Kagoshima University, Japan*
[3] *Laboratory of Molecular Neuroscience, Graduate School of Biological Sciences, Nara Institute of Science and Technology, Japan*

**Correspondence to: Takao Setoguchi, Department of Orthopaedic Surgery, Graduate School of Medical and Dental Sciences, Kagoshima University, 8-35-1 Sakuragaoka, Kagoshima 890-8520, Japan. e-mail: setoro@m2.kufm.kagoshima-u.ac.jp*

Abstract

The Hedgehog pathway functions as an organizer in embryonic development. Aberrant activation of the Hedgehog pathway has been reported in various types of malignant tumours. The GLI2 transcription factor is a key mediator of Hedgehog pathway but its contribution to neoplasia is poorly understood. To establish the role of GLI2 in osteosarcoma, we examined its expression by real-time PCR using biopsy tissues. To examine the function of GLI2, we evaluated the growth of osteosarcoma cells and their cell cycle after *GLI2* knockdown. To study the effect of GLI2 activation, we examined mesenchymal stem cell growth and the cell cycle after forced expression of GLI2. We found that *GLI2* was aberrantly over-expressed in human osteosarcoma biopsy specimens. *GLI2* knockdown by RNA interferences prevented osteosarcoma growth and anchorage-independent growth. Knockdown of *GLI2* promoted the arrest of osteosarcoma cells in G_1 phase and was accompanied by reduced protein expression of the cell cycle accelerators cyclin D1, SKP2 and phosphorylated Rb. On the other hand, knockdown of *GLI2* increased the expression of $p21^{cip1}$. In addition, over-expression of GLI2 promoted mesenchymal stem cell proliferation and accelerated their cell cycle progression. Finally, evaluation of mouse xenograft models showed that *GLI2* knockdown inhibited the growth of osteosarcoma in nude mice. Our findings suggest that inhibition of GLI2 may represent an effective therapeutic approach for patients with osteosarcoma.

Keywords: osteosarcoma; Hedgehog; GLI2; cell cycle

Received 1 October 2010; Revised 12 February 2011; Accepted 20 February 2011

No conflicts of interest were declared.

Introduction

Osteosarcoma is a highly malignant bone tumour and is the most commonly encountered malignant bone tumour in children and adolescents [1,2]. Furthermore, a large number of patients with osteosarcoma eventually develop pulmonary metastases and die, despite conventional multi-agent chemotherapy and surgical excision of the tumour mass [3]. The survival rate of patients treated with intensive multidrug chemotherapy and aggressive local control interventions has been reported to be 60–80% [4,5]. In patients with a high-grade osteosarcoma, the clinical detection of a metastatic disease at first diagnosis is predictive of a poor outcome, with long-term survival rates in the range 10–40% [6]. It has been reported that aberrant activation of cell cycle progression affects the pathogenesis of osteosarcoma [7]. Although inactivation of the deregulated cell cycle seems promising, the molecular mechanisms of osteosarcoma cell growth remain unclear.

Hedgehog–GLI signalling is involved in various steps of development and is induced via the Patched (PTCH1) and Smoothened (SMO) Hedgehog receptors. Activated SMOs promote the translocation of GLI zinc-finger transcription factors into the nucleus [8,9]. In mammals, three transcription factors, viz GLI1, GLI2 and GLI3, activate the transcription of Hedgehog target genes [10,11]. The transcription induced by Gli2 is crucial for development, because *Gli2* knockout mice die prenatally and show defects of the central nervous system [12]. Aberrant activation of Hedgehog pathway is associated with malignant tumours (reviewed in [13]). Our findings indicate that GLI2 is actively involved in the patho-aetiology of osteosarcoma, because suppression of GLI2 inhibits osteosarcoma growth via cell cycle regulation.

Materials and methods

Cell culture

The osteosarcoma cell lines 143B, Saos-2 and HOS were purchased from the American Type Culture Collection (ATCC; Manassas, USA). Osteosarcoma cells

were cultured in Dulbecco's modified Eagle's medium (DMEM) with 10% fetal bovine serum (FBS), penicillin (100 U/ml) and streptomycin (100 μg/ml). The human hTERT-immortalized mesenchymal stem cell line (YKNK-12) was kindly provided by Dr Kobayashi (Okayama University) [14]. YKNK-12 cells were grown in the culture medium described above. Normal human osteoblast cells (NHOsts; Sanko Junyaku, Tokyo, Japan) were grown in OBM™ medium (Cambrex, East Rutherford, NJ, USA). All cells were cultured at 37 °C in a humidified incubator containing 5% CO_2.

Biopsy samples

Human osteosarcoma biopsy tissues were collected from primary lesions before any diagnostic or therapeutic treatment. Control specimens were collected from the femoral bone of patients undergoing total hip arthroplasty. The study protocol was approved by the Review Board of Graduate School of Kagoshima University. Written informed consent was obtained from all patients.

Cell growth assay

The 3-(4,5-dimethylthiazol-2-yl)-2,5-diphenyltetrazolium bromide (MTT) assay was used to evaluate cell proliferation, as previously described [15]. Briefly, cells cultured on microplates were incubated with the MTT substrate for 4 h, and subsequently lysed. The developed optical density of the compound was then analysed using a microplate reader (Bio-Rad, Hercules, CA, USA). GANT61 was obtained from Alexis Biochemicals (CA, USA). The pCS2–MT GLI2ΔN plasmid was provided by Addgene (MA, USA). *GLI2* siRNA was purchased from Santa Cruz Biotechnology (CA, USA). An shRNA plasmid for human *GLI2* was purchased from SA Biosciences (MD, USA). *GLI2* and control shRNAs were cloned into the pGeneClip™ neomycin-resistant vector, which is under the control of the U1 promoter. Transfection of the plasmid was performed according to the supplier's recommendations, using FuGENE6 (Roche, Basel, Switzerland).

Soft agar assay

Cells were suspended in DMEM containing 0.33% soft agar and 5% FBS, and then plated on a 0.5% soft agar layer. The cells were cultured at a density of 5×10^3 cells/well in six-well plates. Fourteen days later, the number of colonies was counted. Every experiment was performed in triplicate, and all experiments were performed three times.

Real-time quantitative PCR assay

Real-time quantitative PCR assay was performed as previously described [16]. Each primer set used amplified a 150–200 bp amplicon. The miR-Vana RNA isolation kit or TRIzol (Invitrogen, Carlsbad, CA, USA) were used for total RNA purification. PCR was performed using SYBR Green as the dye for quantification (Bio-Rad) and analysed using MiniOpticon™ (Bio-Rad). The comparative Ct ($^{\Delta\Delta}$ Ct) analysis method was used to evaluate the fold change of mRNA expression, using the expression of *GAPDH* or *ACTB* as a reference. All PCR reactions were performed in triplicate. All primers were designed using Primer3 software. The following primers were used: *PTCH1*: 5′-TAACGCTGCAACAACTCAGG-3′, 5′-GAAGGCTGTGACATTGCTGA-3′; *SMO*: 5′-GGGAGGCTACTTCCTCATCC-3′, 5′-GGCAGCTGAAGGTAATGAGC-3′; *GLI2*: 5′-CGACACCAGGAAGGAAGGTA-3′, 5′-AGAACGGAGGTAGTGCTCCA-3′; *cyclin D1*: 5′-ACAAACAGATCATCCGCAAACAC-3′, 5′-TGTTGGGGCTCCTCAGGTTC-3′; *SKP2*: 5′-TGGGAATCTTTTCCTGTCTG-3′, 5′-GAACACTGAGACAGTATGCC-3′; *GAPDH*: 5′-GAAGGTGAAGGTCGGAGTC-3′, 5′-GAAGATGGTGATGGGATTTC-3′; *ACTB*: 5′-AGAAAATCTGGCACCACACC-3′, 5′-AGAGGCGTACAGGGATAGCA-3′.

Western blotting

Cells were lysed using NP40 buffer including 0.5% NP40, 10 mM Tris–HCl, pH 7.4, 150 mM NaCl, 3 mM pAPMSF (Wako Chemicals, Kanagawa, Japan), 5 mg/ml aprotinin (Sigma, St Louis, MO, USA), 2 mM sodium orthovanadate (Wako Chemicals, Kanagawa, Japan) and 5 mM EDTA. SDS–PAGE and immunoblotting were subsequently performed and the following antibodies used: GLI2, cyclin D1, p21, SKP2, pRb and actin (Santa Cruz). The ECL reagent was used and chemiluminescence detected (Amersham, Giles, UK).

Plasmid construction

A fragment containing the GLI2ΔN region was obtained from the pCS2-MT GLI2ΔN plasmid (Addgene) and subcloned into the pcDNA3 plasmid.

Luciferase assay

8 × 3′Gli-BS–δ51LucII (GLI–Luc) and 8 × m3′Gli-BS–δ51LucII (mutant-Luc) reporter genes were kindly provided by Dr Sasaki H. [17,18]. Luciferase assays were carried out as described previously [19]. In brief, cells (1.5×10^4 cells/well) were transfected with 400 ng/well of firefly luciferase expression vectors and 1 ng/well internal control vector, pGL4.74 (Promega, Madison, WI, USA) using the FuGENE6 followed by the incubation for 24 h. Recombinant Sonic Hedgehog (R&D Systems, Minneapolis, MO, USA) was added to the well and after 24 h the activities of luciferase were measured, using the Dual-Luciferase Reporter Assay System (Promega) according to the supplier's instructions.